JBC ARTICLE

The hepatokine FGF21 is crucial for peroxisome proliferator-activated receptor-α agonist-induced amelioration of metabolic disorders in obese mice

Received for publication, November 13, 2016, and in revised form, April 12, 2017 Published, Papers in Press, April 12, 2017, DOI 10.1074/jbc.M116.767590

Tsuyoshi Goto[‡§1], Mariko Hirata[‡], Yumeko Aoki[‡], Mari Iwase[‡], Haruya Takahashi[‡], Minji Kim[‡], Yongjia Li[‡], Huei-Fen Jheng[‡], Wataru Nomura[‡§], Nobuyuki Takahashi[‡§], Chu-Sook Kim[¶], Rina Yu[¶2], Shigeto Seno[‖], Hideo Matsuda[‖], Megumi Aizawa-Abe[**], Ken Ebihara[**], Nobuyuki Itoh[‡‡], and Teruo Kawada[‡§]

From the [‡]Laboratory of Molecular Function of Food, Division of Food Science and Biotechnology, Graduate School of Agriculture, Kyoto University, Uji 611-0011, Japan, [§]Research Unit for Physiological Chemistry, Center for the Promotion of Interdisciplinary Education and Research, Kyoto University, Kyoto 606-8501 Japan, [¶]Department of Food Science and Nutrition, University of Ulsan, Ulsan 680-749, South Korea, [‖]Department of Bioinformatic Engineering, Graduate School of Information Science and Technology, Osaka University, Suita 565-0871, Japan, [**]Institute for Advancement of Clinical and Translational Science, Kyoto University Hospital, Kyoto 606-8507, Japan, and [‡‡]Department of Genetic Biochemistry, Kyoto University Graduate School of Pharmaceutical Sciences, Kyoto 606-8501, Japan

Edited by Jeffrey E. Pessin

Obesity causes excess fat accumulation in white adipose tissues (WAT) and also in other insulin-responsive organs such as the skeletal muscle, increasing the risk for insulin resistance, which can lead to obesity-related metabolic disorders. Peroxisome proliferator-activated receptor-α (PPARα) is a master regulator of fatty acid oxidation whose activator is known to improve hyperlipidemia. However, the molecular mechanisms underlying PPARα activator-mediated reduction in adiposity and improvement of metabolic disorders are largely unknown. In this study we investigated the effects of PPARα agonist (fenofibrate) on glucose metabolism dysfunction in obese mice. Fenofibrate treatment reduced adiposity and attenuated obesity-induced dysfunctions of glucose metabolism in obese mice fed a high-fat diet. However, fenofibrate treatment did not improve glucose metabolism in lipodystrophic A-Zip/F1 mice, suggesting that adipose tissue is important for the fenofibrate-mediated amelioration of glucose metabolism, although skeletal muscle actions could not be completely excluded. Moreover, we investigated the role of the hepatokine fibroblast growth factor 21 (FGF21), which regulates energy metabolism in adipose tissue. In WAT of WT mice, but not of FGF21-deficient mice, fenofibrate enhanced the expression of genes related to brown adipocyte functions, such as *Ucp1*, *Pgc1a*, and *Cpt1b*. Fenofibrate increased energy expenditure and attenuated obesity, whole body insulin resistance, and adipocyte dysfunctions in WAT in high-fat-diet-fed WT mice but not in FGF21-deficient mice. These findings indicate that FGF21 is crucial for the fenofibrate-mediated improvement of whole body glucose metabolism in obese mice via the amelioration of WAT dysfunctions.

The rapid increase in the prevalence of obesity and obesity-related chronic diseases including type-2 diabetes, hyperlipidemia, hypertension, and some forms of cancer, is one of the most serious health problems globally (1). Obesity is defined as a state of excessive adiposity, and it occurs when an individual's caloric intake exceeds their energy expenditure. Obesity causes excess fat accumulation not only in white adipose tissues (WATs)[3] but also in other insulin-responsive organs such as the skeletal muscle and the liver, predisposing one to the development of insulin resistance, which can lead to obesity-related metabolic disorders. As of now, the molecular mechanisms underlying obesity and obesity-related metabolic disorders have not been fully clarified, and effective therapeutic approaches are currently of general interest (2).

Peroxisome proliferator-activated receptors (PPARs; PPARα, PPARγ, and PPARδ) are ligand-activated transcription factors belonging to the nuclear hormone receptor superfamily and regulate diverse aspects of whole body lipid and glucose homeostasis and serve as a *bona fide* therapeutic target (3, 4). In particular, PPARα is abundantly expressed in tissues characterized by high rates of fatty acid catabolism, such as the liver, brown adipose tissue (BAT), the heart, and the kidney (5, 6). In these tissues PPARα regulates mRNA expression of genes involved in fatty acid oxidation. Therefore, mice lacking

This work was supported by grants-in-aid for Scientific Research from the Ministry of Education, Culture, Sports, Science, and Technology of Japan (16K07734, 16H02551, 16K12525, and 26280106). The authors declare that they have no conflicts of interest with the contents of this article.

[1] To whom correspondence should be addressed: Laboratory of Molecular Function of Food, Division of Food Science and Biotechnology, Graduate School of Agriculture, Kyoto University, Gokasho, Uji 611-0011, Japan. Tel.: 81-774-38-3753; Fax: 81-774-38-3752; E-mail: tgoto@kais.kyoto-u.ac.jp.

[2] Supported by a grant from the SRC program (Center for Food & Nutritional Genomics Research Grant 2015R1A5A6001906) of the NRF (National Research Foundation) of Korea.

[3] The abbreviations used are: WAT, white adipose tissue; iWAT, inguinal WAT; BAT, brown adipose tissue; UCP1, uncoupling protein 1; PPAR, peroxisome proliferator-activated receptors; FGF21, fibroblast growth factor 21; HFD, high-fat diet; FGFR, FGF receptor; AUC, area under the curve; ACO, acyl-CoA oxidase; CPT1, carnitine palmitoyl transferase 1; HMGCS2, 3-hydroxy-3-methylglutaryl-CoA synthase 2; PGC-1α, PPARγ coactivator-1α; CIDEA, cell death-inducing DNA fragmentation factor α subunit-like effector A; COX4, cytochrome *c* oxidase 4; GLUT1, glucose transporter; AKT, AKT8 virus oncogene cellular homolog.

© 2017 by The American Society for Biochemistry and Molecular Biology, Inc. Published in the U.S.A.

PPARα exhibit higher levels of plasma-free fatty acid and hepatic triglyceride accumulation and severe hypoketonemia under fasting conditions (7). PPARα in hepatocytes is especially important for these phenotypes. Synthetic PPARα agonists, such as fibrates, decrease circulating lipid levels and are commonly used to treat hyperlipidemia and other dyslipidemic states (8). Therefore, PPARα is important for the regulation of whole body lipid metabolism both physiologically and pharmacologically.

PPARα seems to be important for the regulation of not only lipid metabolism but also glucose and energy metabolism. PPARα knock-out mice show excess weight gain with aging and hypoglycemia under fasting conditions (7). Moreover, treatment with PPARα activators attenuate adiposity and adipocyte hypertrophy in animal models of obesity and improve glucose metabolism defects including hyperglycemia, glucose intolerance, and insulin resistance (5, 9–11). However, the molecular mechanisms underlying PPARα activator-mediated reduction in adiposity and improvement of metabolic disorders in the obese state are largely unknown.

Fibroblast growth factor 21 (FGF21) has been reported as a mediator of the pleiotropic actions of PPARα during fasting (12, 13). FGF21 is an atypical member of the FGF family that functions as a hormone to regulate carbohydrate and lipid metabolism. Fasting induced the activation of hepatic PPARα, leading to the direct binding of PPARα to the Fgf21 promoter region followed by the up-regulation of FGF21 (12). FGF21 stimulates hepatic ketogenesis and gluconeogenesis to adapt to fasting (14). Mechanistically, FGF21 activates cell signaling by binding to a heteromeric cell-surface receptor-tyrosine kinase complex composed of β-Klotho and a conventional FGF receptor (FGFR), with FGFR1 being the preferred isoform for FGF21 (15, 16). Both β-Klotho and FGFR1 are abundantly expressed in WAT (17), where FGF21-regulated genes are involved in a variety of metabolic processes, including lipogenesis, lipolysis, and fatty acid oxidation (18, 19). Based on these findings, it was proposed that FGF21 induces futile cycling and energy expenditure in WAT via the enhancement of the BAT function as typified by uncoupling protein 1 (UCP1)-mediated high thermogenic activity in WAT (generally called "browning") (18, 20). Therefore, the function of FGF21 is gathering attention regarding its potential use in the management of obesity and obesity-related metabolic diseases (21). However, the role of FGF21 up-regulated by PPARα agonist in PPARα agonist-mediated amelioration of obesity and obesity-induced metabolic disorders has not been clarified.

In this study we investigated the roles of adipose tissues and FGF21 in PPARα agonist-mediated amelioration of obesity and obesity-induced metabolic disorders. As shown in the results, we showed the pharmacological effects of fenofibrate could be divided into FGF21-dependent effects (anti-obese and anti-abnormalities of glucose metabolism) and FGF21-independent effects (anti-hypertriglyceridemia and hepatomegaly) for the first time. These results indicate that the enhancement of FGF21-induced browning of WAT is important for the PPARα agonist-mediated improvement in energy and glucose metabolism in obese mice. We believe that this study provides important insights into the understanding of the novel mechanism of PPARα activator in the management of glucose metabolism.

Results

Fenofibrate treatment improved obesity and obesity-induced-defective glucose metabolism in diet-induced obese mice

First, we examined whether PPARα agonists affect the development of high-fat diet (HFD)-induced obesity. Fenofibrate treatment significantly attenuated HFD-induced body weight gain (Fig. 1*A*) and adiposity (Table 1) with a slight decrease in food intake (Fig. 1*B*). After 4 weeks of treatment, plasma triglyceride levels in mice treated with fenofibrate were clearly lowered (Fig. 1*C*). Moreover, plasma glucose levels tended to be lower, and obesity-induced hyperinsulinemia was attenuated in mice treated with fenofibrate (Fig. 1*D*). These results indicated that fenofibrate treatment suppressed HFD-induced obesity and the development of glucose metabolism abnormalities in addition to the attenuation of hypertriglyceridemia in mice. Next, to investigate whether fenofibrate treatment affects the diet-induced obesity and obesity-induced glucose metabolism abnormalities, we treated HFD-induced obese mice with fenofibrate for 4 weeks. At the initial treatment, HFD feeding for 12 weeks significantly increased body weight compared with normal-diet (*ND*) feeding (Fig. 1*E*). In this study fenofibrate treatment improved obesity and adiposity despite no significant difference in food intake (Fig. 1, *E* and *F*, Table 2). Oral glucose tolerance tests showed that fenofibrate treatment attenuates obesity-induced glucose intolerance and hyperinsulinemia (Fig. 1, *G* and *H*). After 4 weeks of treatment, obesity-induced hyperglycemia was attenuated by fenofibrate (Fig. 1*I*). Although HFD feeding induced a reduction in plasma FGF21 levels, fenofibrate treatment drastically up-regulated FGF21 levels (Fig. 1*J*). We also checked fenofibric acid, the active metabolite of fenofibrate, specifically activated PPARα among three PPARs subtypes in the reporter assay (Fig. 1*K*).

Fenofibrate treatment did not improve defects in glucose metabolism in lipodystrophic A-Zip/F1 mice

To investigate the role of adipose tissues in fenofibrate-induced amelioration of glucose metabolism defections, lipodystrophic A-Zip/F1 mice were treated with fenofibrate for 4 weeks. A-Zip/F1 mice clearly showed a lipodystrophic phenotype, and we could detect no visible WATs and only a small amount of interscapular BAT (Table 3). As shown in Fig. 2, *A* and *B*, oral glucose tolerance tests and insulin tolerance tests showed lipodystrophic A-Zip/F1 mice presented severe glucose intolerance and insulin resistance, and fenofibrate treatment could not ameliorate glucose intolerance and insulin resistance in A-Zip/F1 mice. After 4 weeks of treatment, fenofibrate improved lipodystrophy-induced hypertriglyceridemia (Fig. 2*D*) but not hyperglycemia (Fig. 2*C*). As reported in the previous report, the liver in A-Zip/F1 mice became more enlarged than in wild-type (WT) mice, and fenofibrate treatment induced enlargement of the liver in A-Zip/F1 mice more potently (Table 3). Plasma FGF21 levels in fenofibrate-treated A-Zip/F1 mice were clearly increased (Fig. 2*E*). Moreover, hepatic mRNA expression levels of PPARα target

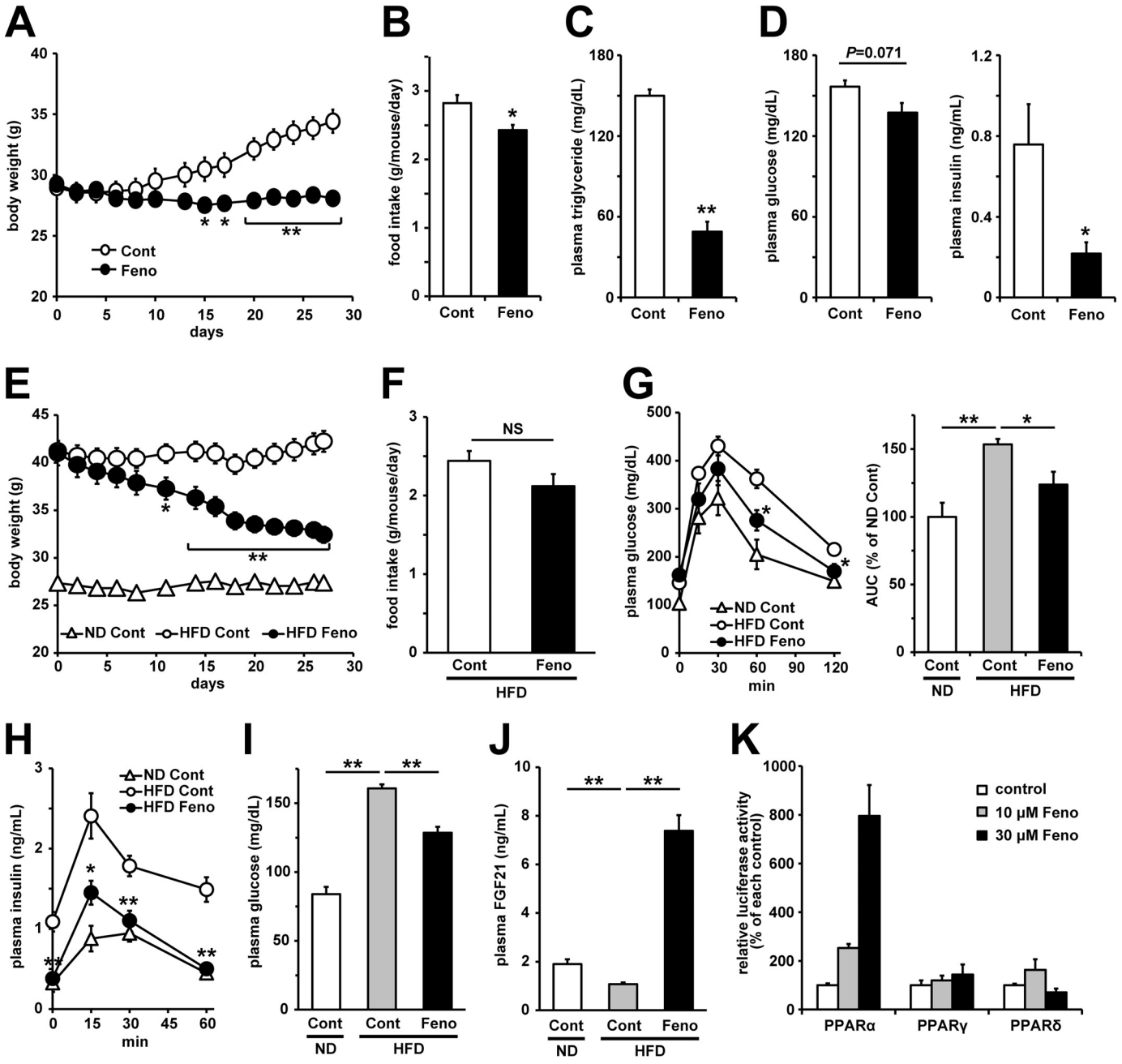

Figure 1. Fenofibrate treatment improved obesity and obesity-induced dysfunctions of glucose metabolism. *A–D*, effects of vehicle (*Cont*, 0.5% carboxymethylcellulose) or fenofibrate (*Feno*, 100 mg/kg/day) treatment for 4 weeks on the development of HFD-induced obesity in C57BL/6J mice. Body weight (*A*), food intake (*B*), plasma triglyceride (*C*), glucose, and insulin (*D*) levels were determined. The values are the means ± S.E. ($n = 4–5$). *E–J*, effects of vehicle or 200 mg/kg/day fenofibrate treatment for 4 weeks on obese C57BL/6J mice fed a HFD for 12 weeks. Body weight (*E*) and food intake (*F*) were measured. Three weeks after the initial treatment, an oral glucose tolerance test (2 g/kg glucose) was performed using mice fasted for 6 h. Plasma glucose levels, the AUC calculated from the plasma glucose curve (*G*) and the plasma insulin levels (*H*) are shown. Four weeks after the initial treatment, plasma glucose levels (*I*) and plasma FGF21 levels (*J*) were measured under a non-fasting state. The values are the means ± S.E. ($n = 6–8$). *K*, ligand activities of fenofibric acid on PPARs were determined by luciferase reporter assay. The values are the means ± S.E. ($n = 3–5$). *, $p < 0.05$; **, $p < 0.01$. *ND*, normal diet; *Cont*, control; *Feno*, fenofibrate (*A–J*) or fenofibric acid (*K*). *NS*, not significant.

genes, including *Fgf21*, *Aco*, *Cpt1a*, and *Hmgcs2*, were upregulated by fenofibrate treatment (Fig. 2*F*). These results clearly showed fenofibrate treatment activated hepatic PPARα, but it could not ameliorate glucose metabolism defects in lipodystrophic A-Zip/F1 mice, suggesting that adipose tissue plays an important role in fenofibrate-induced amelioration of glucose metabolism abnormalities.

Fenofibrate treatment induced the expression of genes related to brown adipocyte function in WAT in WT mice but not in FGF21-deficient mice

Because adipose tissue seemed to play an important role in the fenofibrate-mediated improvement of glucose metabolism abnormalities, we next investigated the role of FGF21, which acts on adipose tissue, leading to anti-obese and anti-diabetic

Table 1

Effects of fenofibrate treatment for 4 weeks on the development of HFD-induced obesity

Values are the means ± S.E. (n = 4–5).

Measurement parameters	Control	Fenofibrate
Body weight (g)	32.7 ± 0.9	26.2 ± 0.4[a]
Inguinal WAT (mg)	1016 ± 93	308 ± 33[a]
Epididymal WAT (mg)	1709 ± 134	499 ± 54[a]
Perireanal WAT (mg)	830 ± 44	181 ± 27[a]
Mesenteric WAT (mg)	496 ± 48	142 ± 14[a]
Interscapular BAT (mg)	96 ± 7	50 ± 4[a]
Liver (mg)	986 ± 27	2028 ± 27[a]
Kidney (mg)	339 ± 12	354 ± 7
Plasma FGF21 (ng/ml)	0.890 ± 0.070	1.850 ± 0.113[a]

[a] $p < 0.01$ compared with the control.

Table 2

Effects of fenofibrate treatment for 4 weeks on the HFD-induced obesity

Values are the means ± S.E. (n = 6–8). ND, normal diet; Cont, control; Feno, fenofibrate.

Measurement parameters	ND Cont	HFD Cont	HFD Feno
Body weight (g)	25.7 ± 0.4	40.6 ± 1.0[a]	30.7 ± 0.8[a,b]
Inguinal WAT (mg)	320 ± 26	2227 ± 173[a]	890 ± 105[a,b]
Epididymal WAT (mg)	484 ± 44	2445 ± 65[a]	1341 ± 124[a,b]
Perireanal WAT (mg)	197 ± 18	1223 ± 68[a]	384 ± 40[a,b]
Mesenteric WAT (mg)	166 ± 21	952 ± 105[a]	225 ± 30[b]
Interscapular BAT (mg)	54 ± 4	103 ± 12[a]	50 ± 3[b]
Liver (mg)	989 ± 29	1093 ± 75	2662 ± 69[a,b]
Kidney (mg)	298 ± 7	357 ± 8	378 ± 6 [a]
Plasma triglyceride (mg/dl)	137.2 ± 2.4	116.4 ± 2.8[c]	44.9 ± 1.6[a,b]

[a] $p < 0.01$ compared with the ND control.
[b] $p < 0.01$ compared with the HFD control.
[c] $P < 0.05$, compared with the ND control.

Table 3

Effects of fenofibrate treatment for 4 weeks on the lipodystrophic A-Zip/F1 mice

Values are the means ± S.E. (n = 4–5). ND, not detectable; Cont, control; Feno, fenofibrate.

		A-Zip/F1	
Measurement parameters	WT Cont	Cont	Feno
Body weight (g)	30.9 ± 1.2	27.8 ± 2.2	28.2 ± 1.9
Inguinal WAT (mg)	330 ± 21	ND	ND
Epididymal WAT (mg)	532 ± 83	ND	ND
Interscapular BAT (mg)	119 ± 9	31 ± 2	22 ± 3
Liver (mg)	1562 ± 88	2792 ± 284	3623 ± 134[a]

[a] $p < 0.05$ compared with the A-Zip/F1 control.

effects (18–20, 22, 23). Two weeks of treatment with fenofibrate under normal diet feeding did not affect food intake (data not shown), body weight, or plasma glucose levels in both WT and FGF21 KO mice (Fig. 3, *A* and *B*). However, fenofibrate treatment did lower plasma triglyceride levels in both genotypes (Fig. 3*C*). In WT mice treated with fenofibrate, plasma FGF21 levels were markedly increased, accompanied with an increase in hepatic *Fgf21* mRNA expression levels (Fig. 3, *D* and *E*). The expression levels of PPARα target genes in the liver, including *Aco*, *Cpt1a*, *Hmgcs2*, and *Cd36*, were up-regulated by fenofibrate treatment to a similar extent in both WT mice and FGF21 KO mice (Fig. 3*E*), suggesting that fenofibrate-induced hepatic PPARα activation seemed not to be affected by FGF21 deficiency. In WAT and BAT, fenofibrate treatment could not induce *Fgf21* mRNA expression levels (Fig. 3, *F* and *G*), suggesting that adipose tissues did not contribute to the fenofibrate-induced enhancement of circular FGF21 levels. In WAT, fenofibrate treatment induced mRNA expression of genes related to brown adipocyte function, such as *Ucp1*, *Pgc1a*, *Cidea*, *Cpt1b*, and *Tbx1* (T-box 1), in WT mice, but these increases were not observed in FGF21 KO mice (Fig. 3*F*). Fenofibrate treatment had no effects on the expression levels of these genes in BAT of both mice genotypes (Fig. 3*G*). Similar to mRNA expression, fenofibrate treatment increased hepatic ACO protein levels in both genotypes and increased UCP1 protein levels in WT mice but not in FGF21 KO mice in WAT (Fig. 3*H*). Moreover, fenofibrate treatment did not affect UCP1 protein expression levels in BAT (Fig. 3*H*). In histochemical analysis, neither fenofibrate treatment nor FGF21 deficiency showed a marked visible effect in the liver or BAT (Fig. 3, *I* and *K*). However, fenofibrate treatment increased the number of small multilocular adipocytes that strongly reacted to UCP1 antibodies only in WAT in WT mice but not in FGF21 KO mice (Fig. 3*J*). Moreover, the cold tolerance test showed fenofibrate treatment significantly ameliorated cold-induced reduction in rectal temperature only in WT mice but not in FGF21 KO mice (Fig. 3*L*), suggesting that fenofibrate induced browning in WAT not only genetically but also functionally. These results suggested that increased hepatic FGF21 production induced by fenofibrate treatment enhances FGF21 signaling in WAT, leading to browning in white adipocytes followed by anti-obese and anti-diabetic effects.

Fenofibrate treatment did not affect the expression of genes related to fatty acid oxidation in skeletal muscle in either WT mice or FGF21-deficient mice

Although WAT and liver are well-known target tissues of FGF21 and PPARα agonist, respectively, several studies indicated that PPARα agonist and FGF21 affect metabolisms in skeletal muscle (24, 25). Therefore, we investigated the effects of fenofibrate treatment on skeletal muscle in WT and FGF21 KO mice. Fenofibrate treatment did not significantly affect mRNA expression levels of PPARα target genes (*Fgf21*, *Aco*, *CpT1b*, and *Lpl*) and the FGF21 target gene (*Glut1*) in skeletal muscle of both genotypes under our experimental conditions (Fig. 4*A*). Tissue distribution of fenofibric acid and *Ppara* expression levels seem to be related to this phenomenon at least partially. The amount of fenofibric acid was ~100 times higher in the liver than in WAT and skeletal muscle (Fig. 4*B*), and *Ppara* was more abundantly expressed in the liver than in WAT and skeletal muscle (Fig. 4*C*). Moreover, the FGF21 sensitivity assay (26, 27) (measurement of FGF21-induced extracellular signal-regulated kinase (ERK) phosphorylation) showed that WAT is more sensitive to FGF21 than the liver and skeletal muscle (Fig. 4*D*). This might be related to the tissue distribution of FGF21 receptors expression. Both *Fgfr1* and *Klb*, which have been shown to be essential for pharmacological activities of FGF21, are more abundantly expressed in WAT than in the liver and skeletal muscle (Fig. 4*E*). These findings indicated that the liver and WAT are the primary target tissues of fenofibrate and FGF21, respectively.

Fenofibrate treatment improved obesity and obesity-induced glucose metabolism abnormalities via the activation of FGF21 signaling

Next, we investigated whether fenofibrate-induced activation of FGF21 signaling in white adipocytes was important for its anti-obese and anti-diabetic activity. To induce obesity, WT

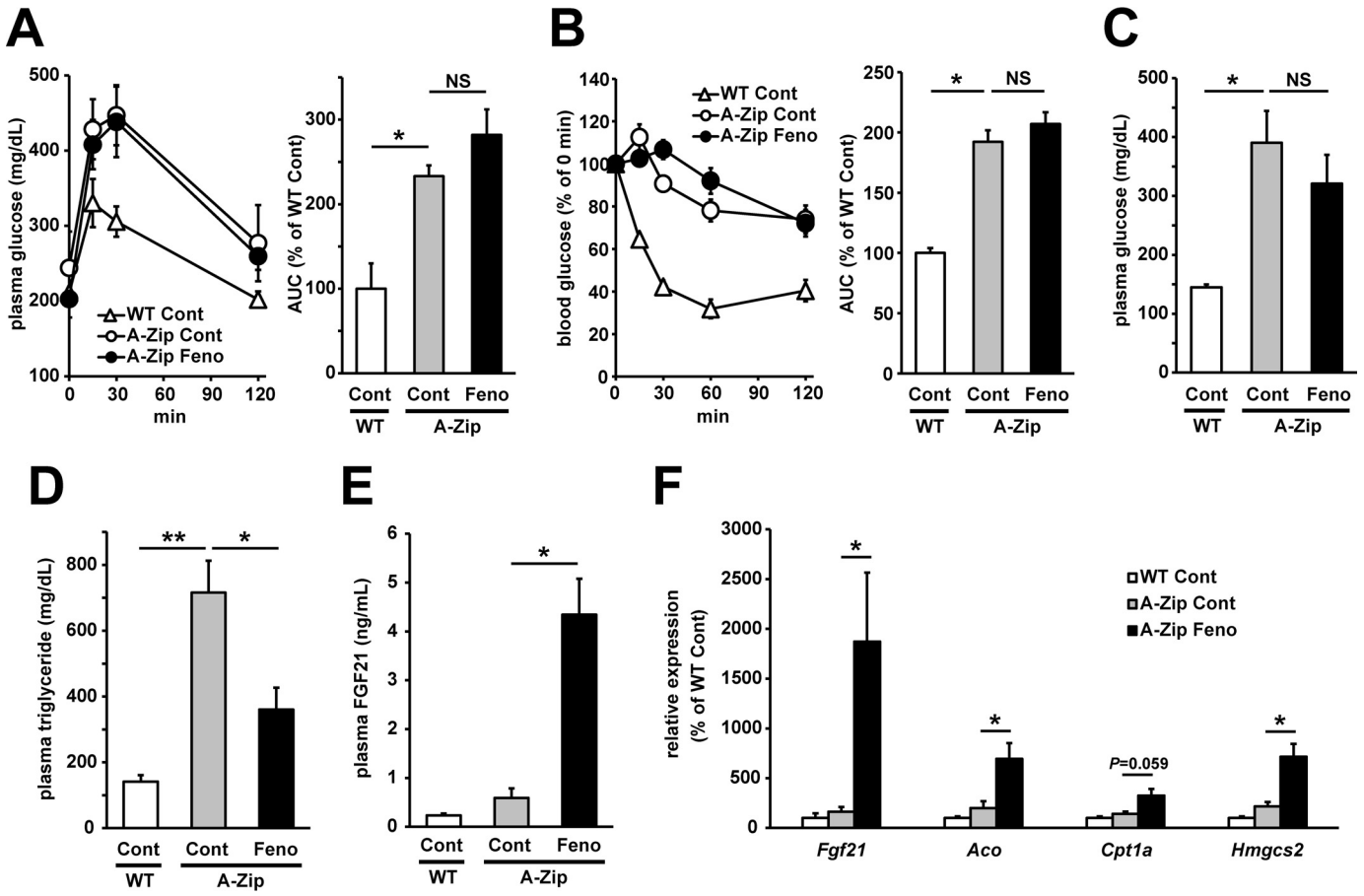

Figure 2. Fenofibrate treatment could improve lipodystrophy-induced hypertriglyceridemia but not glucose metabolism abnormalities in A-Zip/F1 mice. WT mice and lipodystrophic A-Zip/F1 mice were treated with vehicle control or fenofibrate (50 mg/kg/day) for 4 weeks. *A* and *B*, 3 weeks after the initial treatment, the oral glucose tolerance test (*A*) and insulin tolerance test (*B*) were performed using mice fasted for 6 h. Plasma glucose levels and AUC calculated from plasma glucose curve are shown. *C–F*, after 4 weeks of treatment, plasma and liver samples were harvested and analyzed for the measurement of plasma characteristics and mRNA expression levels. Non-fasting plasma glucose levels (*C*), plasma triglyceride levels (*D*), and plasma FGF21 levels (*E*) were determined by enzymatically colorimetric assay or ELISA. The expression levels of hepatic PPARα target genes (*Fgf21*, *Aco*, *Cpt1a*, and *Hmgcs2*) were determined by real-time RT-PCR (*F*). All the values are the means ± S.E. ($n = 4–9$). *, $p < 0.05$; **, $p < 0.01$. *NS*, not significant; *A-Zip*, A-Zip/F1; *Cont*, control; *Feno*, fenofibrate.

and FGF21 KO mice were fed a HFD for 8 weeks. After that, these mice were treated with fenofibrate for 4 weeks. In WT mice, fenofibrate treatment reduced body weight significantly despite no changes in food intake (Fig. 5, *A* and *B*). On the other hand, fenofibrate treatment did not induce a decrease in body weight in FGF21 KO mice even when food intake was slightly decreased (Fig. 5, *A* and *B*). Oxygen consumption rate in both light and dark phase was also increased by fenofibrate treatment in WT mice but not in FGF21 KO mice, suggesting that fenofibrate-mediated reduction in body weight in WT mice was at least partially due to an enhancement of energy expenditure (Fig. 5*C*). After 4 weeks of treatment, fenofibrate treatment more clearly and significantly reduced adipose tissue weight in WT mice, although adipose tissue weight tended to be lower in FGF21 KO mice treated with fenofibrate (Table 4). Plasma glucose levels were significantly decreased only in WT mice by fenofibrate treatment, accompanied with the enhancement of circular FGF21 levels, whereas fenofibrate treatment decreased plasma triglyceride levels in both genotypes (Table 4). Moreover, fenofibrate also induced hepatomegaly in both genotypes (Table 4), suggesting that FGF21 is not essential for fenofibrate-induced anti-hypertriglyceridemia effect and hepatomegaly. Oral glucose tolerance tests showed that fenofibrate treatment markedly improved glucose tolerance and hyperinsulinemia in WT mice, whereas the amelioration of glucose intolerance and hyperinsulinemia was clearly limited in FGF21 KO mice (Fig. 5*D*). Insulin tolerance tests clearly showed that insulin resistance was improved in WT mice treated with fenofibrate, but this amelioration was not observed in FGF21 KO mice (Fig. 5*E*). These results clearly showed that FGF21 plays an important role in fenofibrate-induced improvement of obesity and glucose metabolism abnormalities but not fenofibrate-induced improvement of hypertriglyceridemia.

Fenofibrate treatment attenuated obesity-induced WAT dysfunction in WT mice

We assessed the effects of fenofibrate treatment on obesity-induced tissue dysfunctions. We could not observe marked visible changes in hepatic histological analysis or differences in hepatic triglyceride accumulation by fenofibrate treatment and FGF21 deficiency (Fig. 6*A*). Next, to assess the effects of fenofibrate treatment on obesity-induced WAT dysfunction, we investigated adipocyte size in WAT. In WT mice, fenofibrate treatment suppressed obesity-induced adipocyte hypertrophy.

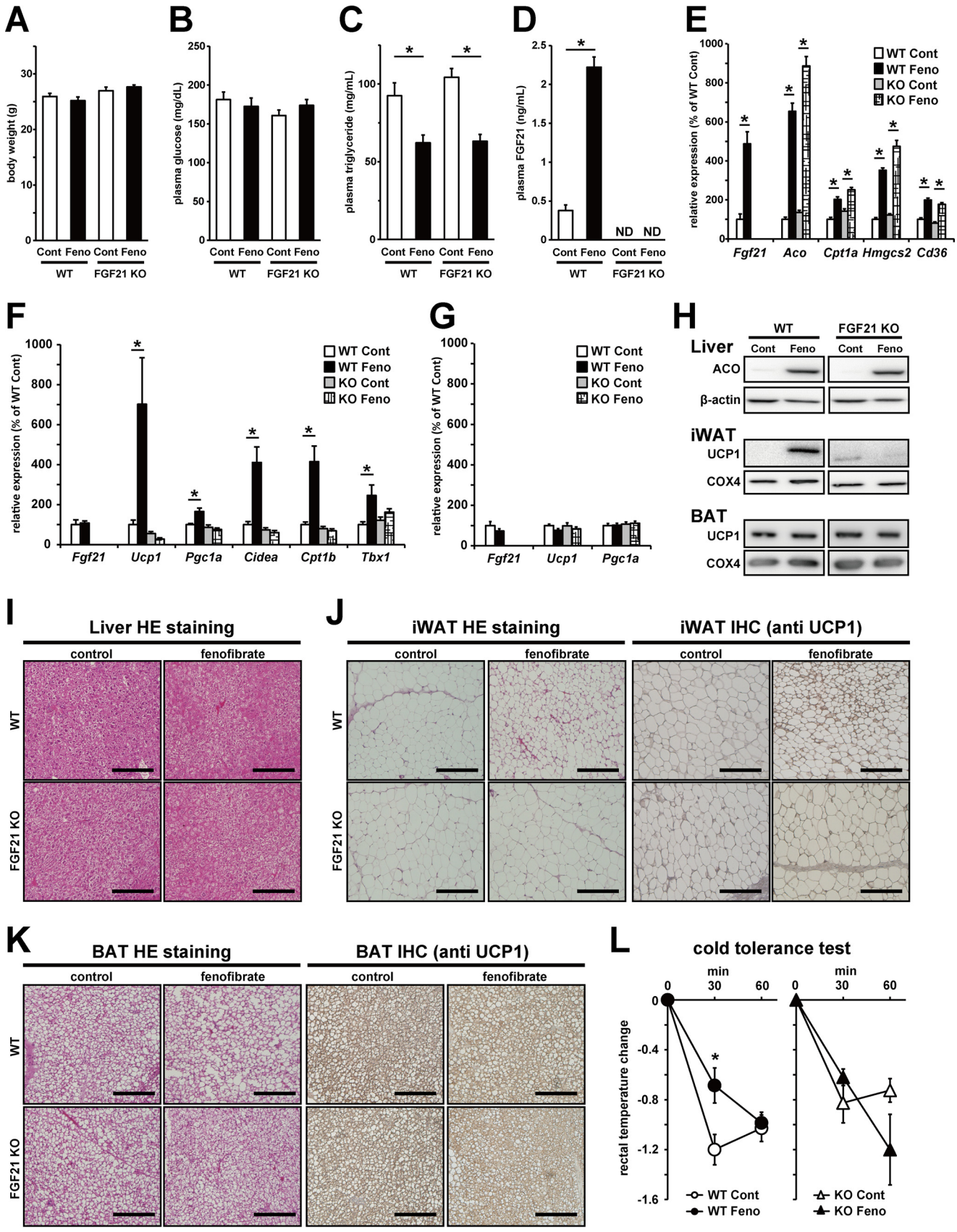
A
body weight (g)
Cont Feno Cont Feno
WT FGF21 KO
B
plasma glucose (mg/dL)
C
plasma triglyceride (mg/mL)
D
plasma FGF21 (ng/mL)
ND ND
E
relative expression (% of WT Cont)
WT Cont
WT Feno
KO Cont
KO Feno
Fgf21 Aco Cpt1a Hmgcs2 Cd36
F
Fgf21 Ucp1 Pgc1a Cidea Cpt1b Tbx1
G
Fgf21 Ucp1 Pgc1a
H
WT
FGF21 KO
Liver
ACO
β-actin
iWAT
UCP1
COX4
BAT
UCP1
COX4
I
Liver HE staining
control
fenofibrate
WT
FGF21 KO
J
iWAT HE staining
iWAT IHC (anti UCP1)
K
BAT HE staining
BAT IHC (anti UCP1)
L
cold tolerance test
min
rectal temperature change
WT Cont
WT Feno
KO Cont
KO Feno

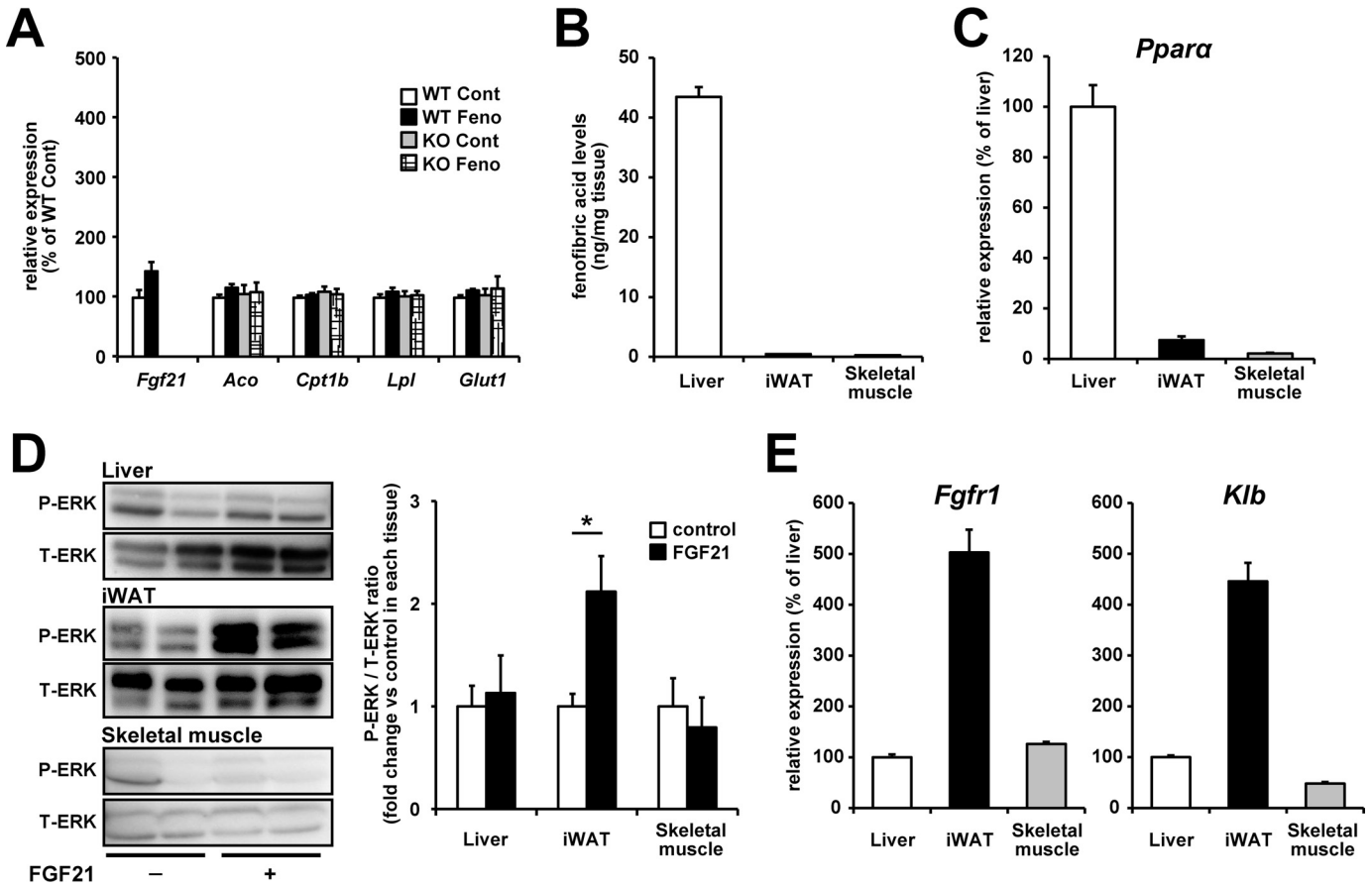

Figure 4. Fenofibrate treatment did not affect the expression of genes related to fatty acid oxidation in skeletal muscle in either WT mice or FGF21-deficient mice. *A* and *B*, 10-week-old C57BL/6J WT mice and FGF21 KO mice were treated with vehicle control or 50 mg/kg/day fenofibrate for 2 weeks. mRNA expression levels of PPARα target genes (*Fgf21*, *Aco*, *Cpt1b*, and *Lpl*) and FGF21 target gene (*Glut1*) in the skeletal muscle (gastrocnemius) were determined by real-time RT-PCR (*A*). The contents of fenofibric acid in each tissue sample were quantified by LC-MS (*B*). *C–E*, 8-week-old C57BL/6J mice were used for analysis of mRNA expression levels of *Ppara* (*C*) and main FGF21 receptors (*Fgfr1* and *Klb*) (*E*) and the FGF21 sensitivity assay (25 μg/kg recombinant FGF21, i.p.) (*D*). The values are the means ± S.E. ($n = 3–4$). *, $p < 0.05$. *P-ERK*, phosphorylated ERK; *T-ERK*, total ERK.

However, this effect was not observed in FGF21 KO mice (Fig. 6, *B–D*). Moreover, insulin injection obviously enhanced AKT phosphorylation in WAT in fenofibrate-treated WT mice compared with vehicle-treated WT mice. On the other hand, fenofibrate-mediated enhancement of AKT phosphorylation was not observed in FGF21 KO mice (Fig. 6*E*), suggesting FGF21 was important for the fenofibrate-induced improvement of obesity-induced insulin resistance in adipocytes. Insulin-stimulated AKT phosphorylation also tended to be enhanced in the liver and skeletal muscle only in WT mice by fenofibrate treatment (Fig. 6, *F* and *G*), but fenofibrate-enhanced insulin-stimulated AKT phosphorylation was observed more clearly in WAT. These results indicate that fenofibrate treatment improves obesity-induced WAT dysfunction, such as adipocyte hypertrophy and insulin resistance in adipocytes, and FGF21 played an important role in delivering these effects of fenofibrate. We did not observe significant differences of plasma free fatty acids and adiponectin levels (Table 4).

FGF21 played an important role in fenofibrate-induced browning in WAT

Finally, we investigated the effects of fenofibrate treatment on mRNA and protein expression levels in the liver, WAT, and BAT in HFD-induced obese mice. As previously reported (28), mRNA expression of FGF21 was up-regulated by fenofibrate treatment only in the liver of these organs (Fig. 7*A*–7C), suggesting that the liver is an important organ for the increase in circular FGF21 levels in obese mice. mRNA and protein expression levels of PPARα target genes related

Figure 3. Fenofibrate treatment induced mRNA and protein expression levels of genes related to brown adipocyte function in WAT of WT mice but not in FGF21 KO mice. *A–K*, 12-week-old C57BL/6J WT mice and FGF21 KO mice were treated with vehicle control or 50 mg/kg/day fenofibrate for 2–3 weeks. After 2 weeks of treatment, plasma, liver, iWAT, and BAT were harvested and analyzed for the measurement of plasma characteristics, mRNA expression levels, and protein expression levels. *A*, body weight was measured after 2 weeks of fenofibrate treatment. *B–D*, plasma glucose (*B*), triglyceride (*C*), and FGF21 (*D*) levels were determined by enzymatic colorimetric assay or ELISA. *E–G*, mRNA expression levels of PPARα target genes in the liver (*E*) or genes related to brown adipocyte functions in iWAT (*F*) and BAT (*G*) were determined by real-time RT-PCR. *H*, protein expression levels of ACO, UCP1, and β-actin in total proteins from the liver or BAT and UCP1 and COX4 in mitochondrial proteins from iWAT or BAT were analyzed by Western blotting. *I–K*, histochemical analyses of the liver (*I*), iWAT (*J*), and BAT (*K*) were performed by hematoxylin and eosin (*HE*) staining or immunohistochemical (*IHC*) staining using the antibody against UCP1. *Scale bars* in the panels represent 200 μm. *L*, changes of rectal temperature in the cold tolerance test are shown. All the values are the means ± S.E. ($n = 4–10$). *, $p < 0.05$. *ND*, not detectable; *Cont*, control; *Feno*, fenofibrate.

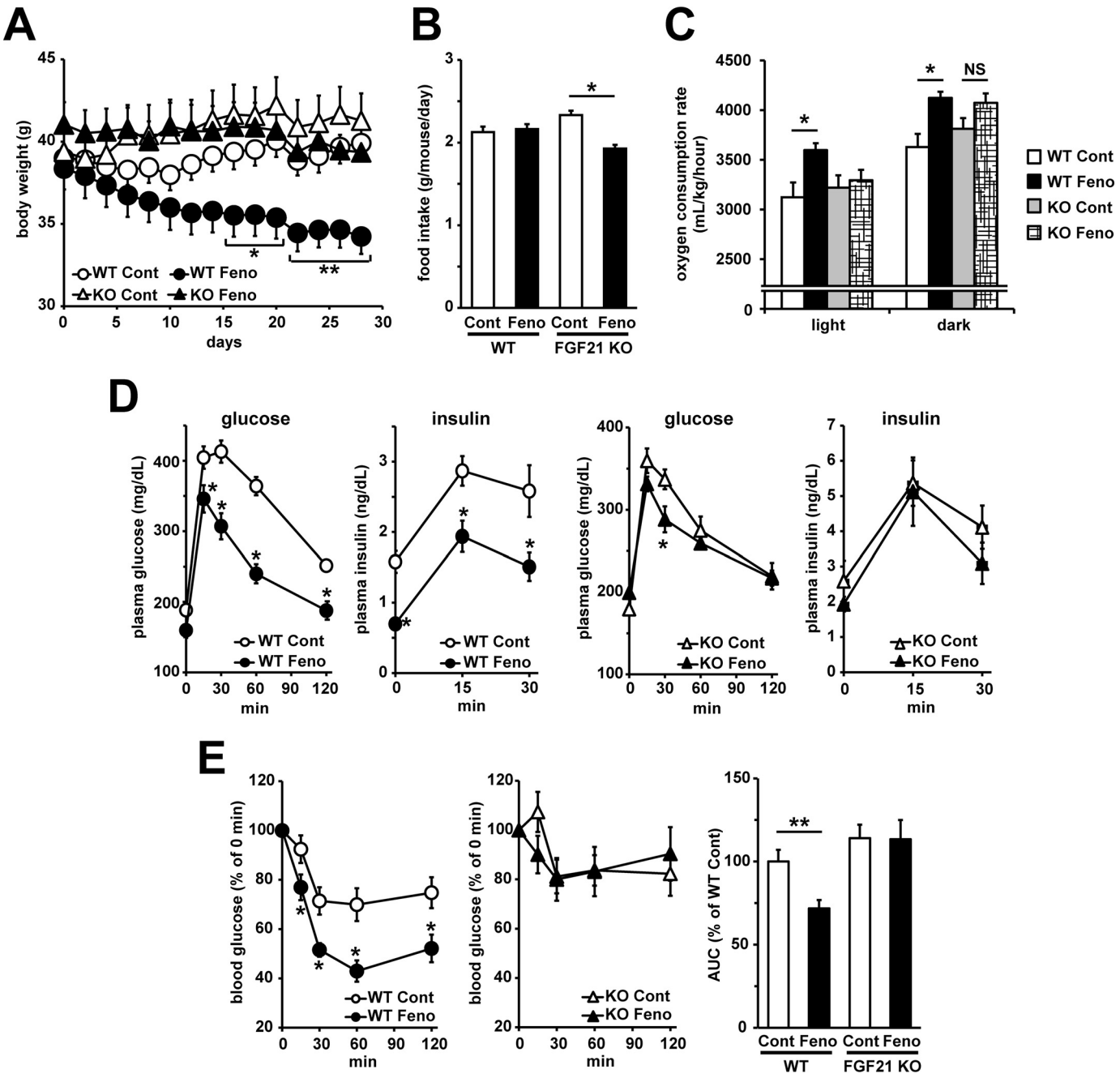

Figure 5. FGF21 was important for the fenofibrate-mediated amelioration of glucose metabolism dysfunctions induced by obesity. Seven-week-old C57BL/6J WT mice and FGF21 KO mice fed a HFD for 8 weeks were subjected to 4 weeks of fenofibrate treatment (50 mg/kg/day) under HFD feeding. *A* and *B*, body weight (*A*) and food intake were measured. *C*, 3 weeks after treatment, oxygen consumption rate was measured by indirect calorimetric system under the fed condition for 20 h (light phase: 8 h; dark phase: 12 h). *D*, three weeks after treatment, a oral glucose tolerance test (2 g/kg glucose) was performed after 6 h of fasting. Plasma glucose levels and insulin levels were determined by enzymatically colorimetric assay or ELISA, respectively. *E*, 3 weeks after treatment, an insulin tolerance test (1 unit/kg insulin, i.p.) was performed after 6 h fasting. Plasma glucose levels determined by enzymatically colorimetric assay, and the AUC calculated from plasma glucose curve are shown. All values are the means ± S.E. ($n = 4–8$). *, $p < 0.05$; **, $p < 0.01$. *NS*, not significant; *Cont*, control; *Feno*, fenofibrate.

to fatty acid oxidation in the liver were up-regulated by fenofibrate treatment to the same extent in both WT and FGF21 KO mice (Fig. 7, *A* and *D*). Moreover, plasma β-hydroxybutyrate levels were elevated by fenofibrate treatment in both genotypes, suggesting that hepatic fatty acid oxidation was enhanced by fenofibrate treatment in both genotypes (Table 4). However, mRNA and protein expression levels of the genes related to brown adipocytes function were only up-regulated by fenofibrate in the WAT of WT mice, and this fenofibrate-induced up-regulation was not observed in BAT of WT mice and WAT and BAT of FGF21 KO mice (Fig. 7, *B* and *C*), suggesting that FGF21 plays an important role in the up-regulation of brown adipocyte-related genes in WAT by fenofibrate treatment, and this FGF21-mediated induction of browning in WAT may be important for anti-obese and anti-diabetic phenotypes in mice treated with fenofibrate.

Table 4
Effects of fenofibrate treatment for 4 weeks on HFD-induced obese C57BL/6 WT and FGF21 KO mice
Values are the means ± S.E. (n = 7–8). ND, not detectable; Cont, control; Feno, fenofibrate.

	WT		FGF21 KO	
Measurement parameters	Cont	Feno	Cont	Feno
Body weight (g)	39.3 ± 1.11	34.2 ± 1.06[a]	41.3 ± 1.78	39.4 ± 1.39
Inguinal WAT (mg)	1200 ± 120	731 ± 106[a]	1299 ± 65	1171 ± 128
Epididymal WAT (mg)	2174 ± 152	1425 ± 219[b]	1908 ± 113	1641 ± 94
Perireanal WAT (mg)	1079 ± 64	599 ± 94[a]	1074 ± 77	815 ± 73[b]
Interscapular BAT (mg)	86 ± 10	70 ± 9	85 ± 7	69 ± 7
Kidney (mg)	364 ± 11	407 ± 10[b]	411 ± 19	433 ± 16
Liver (mg)	1416 ± 82	2358 ± 97[a]	1562 ± 199	2523 ± 214[a]
Plasma characteristics				
Glucose (mg/dl)	206 ± 9.1	174 ± 4.6[b]	191 ± 6.1	177 ± 7.4
Triglyceride (mg/dl)	79 ± 3.8	49 ± 2.1[a]	79 ± 5.9	53 ± 2.5[b]
β-Hydroxybutyrate (μM)	51.0 ± 12.1	111 ± 21.4[b]	51.8 ± 10.1	138 ± 27.2[b]
Free fatty acids (meq/liter)	1.03 ± 0.049	0.91 ± 0.040	0.87 ± 0.029	0.95 ± 0.067
FGF21 (ng/ml)	0.351 ± 0.03	2.51 ± 0.28[a]	ND	ND
Adiponectin (μg/ml)	56.2 ± 3.0	46.3 ± 4.4	58.1 ± 5.0	54.5 ± 7.1

[a] $p < 0.01$ compared with the control in each genotype.
[b] $p < 0.05$, compared with the control in each genotype.

Discussion

In rodents, treatment with PPARα agonist has been reported to suppress obesity and obesity-induced abnormalities in glucose metabolism (5, 9–11). In humans, several reports have indicated that PPARα agonists, fibrates, might be useful for the management of disorders in glucose metabolism in non-insulin-dependent diabetes mellitus (29–32). Moreover, the observation that certain PPARα genetic polymorphisms may delay the development of type 2 diabetes in humans supports the hypothesis that PPARα activator could increase insulin sensitivity in humans (33). Moreover, PPARα agonist treatment enhanced circular FGF21 levels not only in rodents but also humans (34), suggesting that PPARα agonist treatment could enhance FGF21 signaling in human adipose tissue. Moreover, treatment with LY2405319, an FGF21 analog in obese human subjects with type 2 diabetes, resulted in favorable effects on body weight, fasting insulin, and hyperlipidemia (21). These reports raise the possibility that PPARα agonist-induced activation of FGF21 signaling might be effective against disorders of energy and glucose metabolism in human.

BAT is specialized in oxidizing lipids to dissipate chemical energy in the form of heat in a process called adaptive thermogenesis (35). Mitochondrial UCP1 in BAT generates heat through the uncoupling of oxidative phosphorylation (36). BAT activity is inversely correlated with body mass index and adiposity (37–39), indicating that controlling BAT activity could be used to protect against obesity and obesity-related metabolic disorders. Unlike classical brown adipocytes, which arise from muscle-like type progenitors (35), UCP1-expressing, brown-like adipocytes (generally called beige cells or bright adipocytes) emerge in WAT under certain physiological and pharmacological conditions, such as cold stimulation and β-adrenoreceptor agonists (40, 41). Recent genome-wide analyses of isolated clonal UCP1-positive adipocytes from adult human BAT indicated that cloned human brown adipocytes have molecular signatures that resemble murine beige cells rather than classical brown adipocytes (42). Moreover, chronic cold acclimation results in recruitment of new BAT in adult humans who do not possess detectable BAT before treatment (43, 44). These reports indicate that inducible UCP1-expressing beige cells play important roles in the regulation of energy metabolisms in both rodents and humans. In this study fenofibrate treatment induced the expression of genes related to brown adipocyte functions, such as *Ucp1* and *Pgc1a*, in inguinal white adipose tissue but not in brown adipose tissue, suggesting that fenofibrate treatment predominantly enhances the function of inducible UCP1-expressing, brown-like adipocytes under our experimental conditions. FGF21 treatment more potently induced *Ucp1* and *Pgc1a* expression in inguinal WAT (iWAT) than in BAT. Moreover, although differences in cold-induced thermogenic gene expression were not apparent in the interscapular BAT of FGF21-KO mice, the expression of browning marker genes, such as *Ucp1*, *Pgc1a*, *Cidea*, was significantly reduced in the iWAT of the cold-exposed FGF21-KO mice (20). Therefore, activation of FGF21 signaling may enhance BAT function more efficiently in iWAT than BAT.

PPARα is predominantly expressed in the liver, and hepatic PPARα plays an essential role in many physiological functions of PPARα, such as fasting-induced hepatic lipid accumulation and the maintenance of whole body fatty acid metabolisms. PPARα is also expressed in WAT, and several reports have shown that direct activation of PPARα in white adipocytes can regulate white adipocyte function (5, 10, 45–47). PPARα activation in white adipocytes induced an anti-diabetic and anti-atherosclerosis hormone adiponectin expression and secretion levels via direct binding to the adiponectin promoter region (45). Mazzucotelli *et al.* (46) report that PPARα activation in human white adipocytes controls the expression of metabolism genes including glycerol kinase independently of PPARγ. Moreover, several reports indicate PPARα activation in white adipocyte enhanced β-oxidation gene expression and increased fatty acid oxidation activity and oxygen consumption rate (5, 47). Because high capacity of fatty acid oxidation and oxygen consumption is one of the major features of brown adipocytes (48), PPARα agonist may directly induce browning in white adipocyte. However, we did not observe fenofibrate treatment-induced browning in FGF21 KO mice, suggesting that fenofibrate-induced direct activation of PPARα in white adipocytes seems not to be involved in the WAT remodeling under our experimental conditions. As shown in Fig. 4*B*, pharmacological

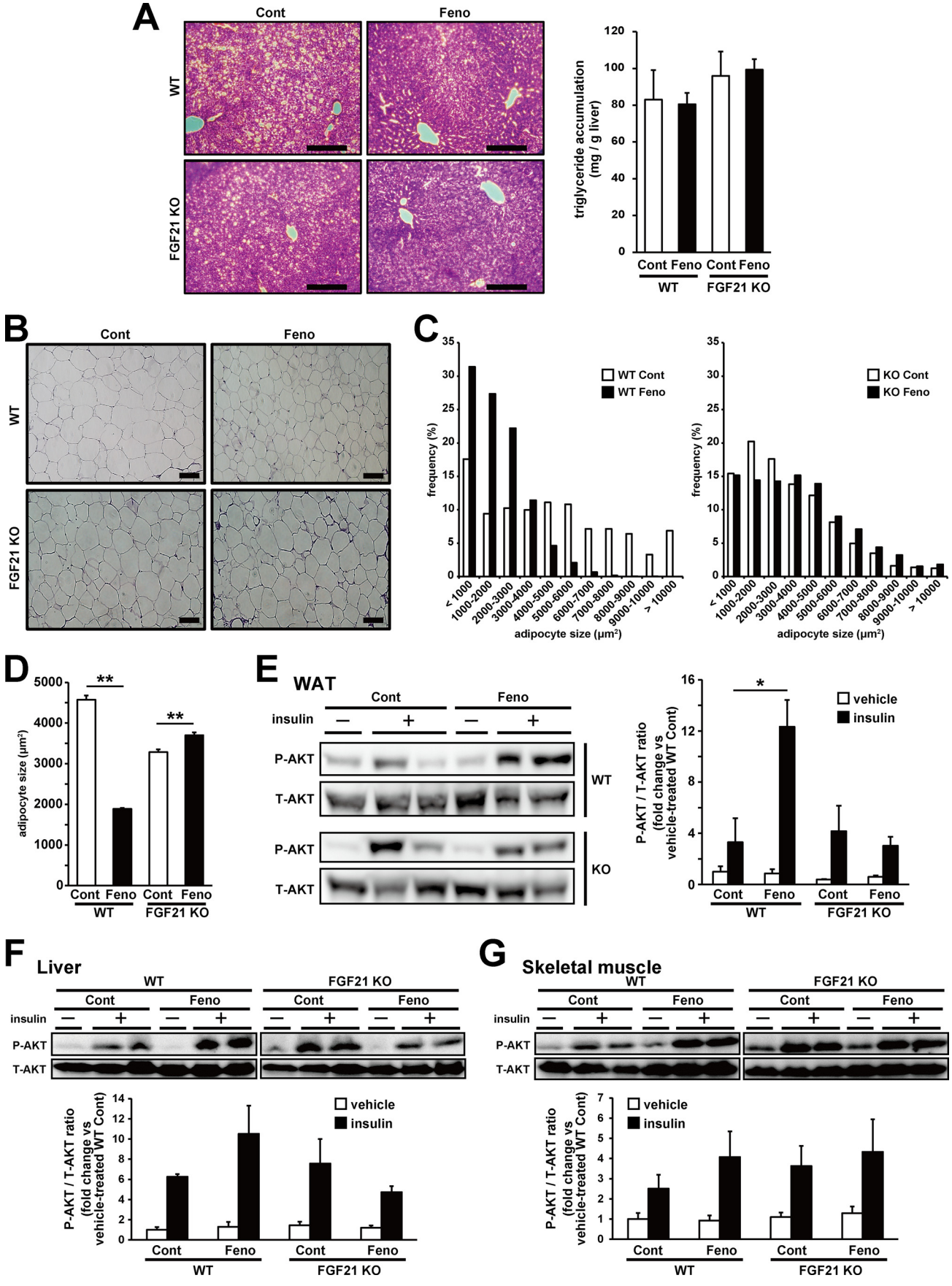
A
Cont
Feno
WT
FGF21 KO
triglyceride accumulation (mg / g liver)
Cont Feno Cont Feno
WT
FGF21 KO
B
C
WT Cont
WT Feno
KO Cont
KO Feno
frequency (%)
adipocyte size (μm²)
D
adipocyte size (μm²)
E
WAT
insulin
P-AKT
T-AKT
P-AKT / T-AKT ratio (fold change vs vehicle-treated WT Cont)
vehicle
insulin
F
Liver
G
Skeletal muscle

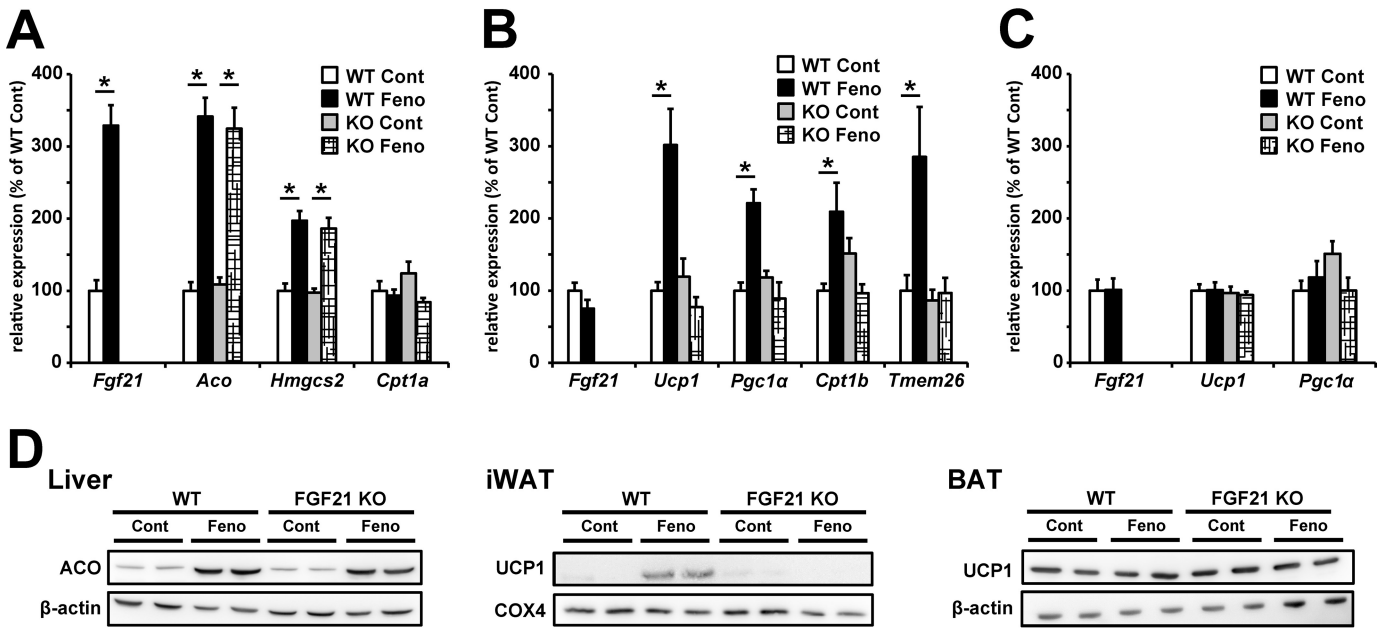

Figure 7. FGF21 was important for fenofibrate-induced browning in WAT. Seven-week-old C57BL/6J WT mice and FGF21 KO mice fed HFD for 8 weeks were subjected to fenofibrate treatment (50 mg/kg/day) under HFD feeding. After 4 weeks of treatment, liver, WAT, and BAT were removed and mRNA and protein expression were analyzed. *A-C*, mRNA expression levels of PPARα target genes in the liver (*A*) and mRNA expression levels of the genes related to brown adipocyte function in WAT (*B*) and BAT (*C*) were determined by real-time RT-PCR. Protein expression levels of ACO, UCP1, and β-actin in total proteins from the liver or BAT and UCP1 and COX4 in mitochondrial proteins from WAT were analyzed using Western blotting. All values are the means ± S.E. ($n = 8–10$). *, $p < 0.05$. *Cont*, control; *Feno*, fenofibrate.

properties of fenofibrate might have a profound effect on the results of our study. Therefore, a PPARα activator efficiently delivered to liver and adipose tissue may synergistically enhance BAT function via not only increased FGF21 production in the liver but also direct activation of PPARα in adipocytes.

Recent studies have shown that FGF21 production in adipocytes is stimulated by many stimuli, such as cold exposure and PPARγ agonist (20, 28). Cold exposure induced FGF21 expression levels in both brown and white adipose tissues, leading to the enhancement of brown adipocyte function in these tissues (20). Under cold temperatures, noradrenaline, acting via β-adrenergic, cAMP-mediated, mechanisms, and subsequent activation of protein kinase A and p38 MAPK seems to induce FGF21 gene transcription and FGF21 secretion (49). Cold-induced enhancement of brown adipocyte function was impaired in both BAT and WAT of FGF21-deficient mice, indicating that FGF21 enhances brown adipocyte function in adipose tissues in an autocrine/paracrine manner (20). In humans, cold exposure increased circulating FGF21 levels, which induced brown adipocyte-related gene expression in adipocytes, enhancing lipolysis and thermogenesis response (50, 51). Adipocyte FGF21 signaling has been reported to be important not only for the induction of thermogenic activity but also the regulation of insulin sensitivity in WAT (28). FGF21 could regulate activity of PPARγ, a master transcriptional regulator of adipogenesis, via the suppression of sumoylation of PPARγ, which reduces its transcriptional activity. Furthermore, FGF21 is a potent regulator of adiponectin (52, 53). Therefore, fenofibrate-induced activation of FGF21 signaling in WAT could ameliorate obesity-induced WAT abnormalities multilaterally.

FGF21 activates cellular signaling by binding its cell surface receptors FGFR1 and β-Klotho, which are abundantly expressed in adipocytes. Therefore, most pharmacological functions of FGF21 treatment, such as the lowering of plasma glucose, insulin, and triglycerides and increases in energy expenditure were diminished in adipose FGFR1 knock-out mice (22). Moreover, FGF21-mimicking antibody-mediated amelioration of glucose metabolism disorders was shown in obese db/db mice but not in lipodystrophic mice (23). These reports clearly indicated that adipose tissue plays an essential role in FGF21-mediated amelioration of metabolic disorders. In this study, fenofibrate treatment had beneficial effects on hypertriglyceridemia in lipodystrophic A-Zip/F1 mice and diet-induced obese FGF21 KO mice. Therefore, FGF21 signaling in adipocytes seems not to be involved in PPARα agonist-mediated circular triglyceride-lowering effect. Fenofibrate could induce hepatic fatty acid oxidation-related PPARα target

Figure 6. FGF21 was important for fenofibrate-induced amelioration of adipose tissue dysfunction induced by obesity. Seven-week old C57BL/6J WT mice and FGF21 KO mice fed HFD for 8 weeks were subjected to the fenofibrate treatment (50 mg/kg/day) under HFD feeding. After 4 weeks of treatment, tissues were removed and analyzed. *A–D*, liver (*A*) and WAT (*B*) samples embedded in the paraffin were cut into 6-μm sections. Each section was stained with hematoxylin and eosin. Representative images of liver sections are shown (*scale bars* in the *panels* represent 200 μm), and hepatic triglyceride contents were measured by an enzymatically colorimetric assay (*A*). Representative images of WAT sections are shown, and *scale bars* in the *panels* represent 100 μm (*B*). Distribution (*C*) and average (*D*) of the adipocyte size were determined by image analysis. All values are the means ± S.E. ($n = 1063–3125$). *E–G*, human insulin was injected intraperitoneally (2 units/kg) into mice fasted overnight. WAT (*E*), liver (*F*), and skeletal muscle (gastrocnemius) (*G*) were harvested from mice, and AKT phosphorylation levels were determined using immunoblotting. Protein bands were quantified by image analysis. All values are the means ± S.E. ($n = 3–4$). *, $p < 0.05$; **, $p < 0.01$. Cont, control; Feno, fenofibrate. *P-AKT*, phosphorylated AKT; *T-AKT*, total AKT.

gene expression in FGF21 KO mice to the same extent as in WT mice under our experimental conditions. This indicates that FGF21 is not essential for fenofibrate-enhanced fatty acid oxidation in the liver, although FGF21 could induce PGC-1α-mediated fatty acid oxidation in the liver under fasting conditions (14). It is likely that FGF21-independent fenofibrate-mediated activation of fatty acid oxidation in the liver is enough to lower plasma triglyceride levels.

Consistent with previous studies, fenofibrate treatment induces hepatomegaly without triglyceride accumulation in this study (54, 55). It has been reported that prolonged PPARα agonist treatment in rodents induces hepatocellular proliferation and suppresses hepatocyte apoptosis leading to hepatomegaly (56). More recently, it was shown that PPARα agonist treatment induces hepatomegaly via the activation of PPARα in hepatocytes using hepatocyte-specific PPARα-deficient mice (7, 57). FGF21 has been reported not to induce proliferation of cells typically sensitive to FGFs (58). Moreover, in our study, fenofibrate treatment induced hepatomegaly in both WT mice and FGF21 KO mice at a similar level (Table 4), suggesting that FGF21 was not involved in the PPARα agonist-induced hepatocyte proliferation.

Insulin resistance in skeletal muscle promotes the development of the metabolic abnormalities (59). In this study insulin-stimulated AKT phosphorylation in skeletal muscle tended to be increased by fenofibrate treatment only in WT mice but not in FGF21 KO mice. Moreover, several studies have reported skeletal muscle could be direct target organs of the PPARα agonist (24) and FGF21 (25). However, fenofibrate treatment did not affect mRNA expression levels of PPARα target genes and the FGF21 target gene in either WT mice or FGF21 KO mice, suggesting that skeletal muscle did not function as the target organ of fenofibrate and fenofibrate-stimulated FGF21 under our experimental conditions. This might be caused by the pharmacological properties of fenofibrate; that is, lower expression levels of *Ppara* and Fgf21 receptors in skeletal muscle as shown in Fig. 4.

In this study fenofibrate treatment sometimes, but not always, reduced food intake significantly (Figs. 1*B* and *F*, and 5*B*). We do not understand this difference. However, the relationship between the activation of PPARα and food intake might be very complicated. Several previous studies reported PPARα agonist treatment did not affect food intake in rodents even at 500 mg/kg fenofibrate treatment (0.5% fenofibrate diet (~500 mg/kg) (55) and 500 mg/kg fenofibrate (60)), which is a much higher dose than the doses used in this study. However, there are reports in which PPARα activation in rodents caused the reduction in food intake (10, 61). These previous studies indicated the subtle differences in the experimental conditions could affect the relationship between the activation of PPARα and food intake. However, previous study showed that PPARα agonist treatment improved obesity even under pair-fed conditions (10), suggesting that enhancement of energy expenditure is important for the anti-obesity effect of PPARα agonist, at least partially. Therefore, we believe the PPARα agonist-FGF21-WAT browning pathway contributes to the anti-obesity effect of PPARα agonist.

In conclusion, in this study we showed that fenofibrate treatment could ameliorate obesity and obesity-related glucose metabolism disorders in diet-induced obese mice, whereas hyperglycemia and glucose intolerance in lipodystrophic mice was not ameliorated by fenofibrate treatment. Thermogenic functions in WAT of mice treated with fenofibrate seemed to be enhanced via the increase in hepatic FGF21 production, leading to the amelioration of obesity-induced WAT dysfunction accompanied with the enhancement of whole body insulin sensitivity. On the other hand, the fenofibrate-induced plasma triglyceride lowering effect and hepatomegaly were independent on the FGF21 function. These findings may provide us with new insight into the pharmacological usefulness of fibrate drugs.

Experimental procedures

Materials and methods

Unless otherwise indicated, all chemicals used were purchased from Sigma, Nacalai Tesque (Kyoto, Japan), or Wako (Osaka, Japan) and were guaranteed to be of reagent or tissue culture grade.

Animals

All mice were housed under a constant 12-h light/dark cycle with free access to food and water. For the diet-induced obese model, 7–8-week-old wild type C57BL/6J mice (Japan SLC, Shizuoka, Japan) or FGF21-deficient mice (62) were fed a 60% HFD (D12492; Research Diet). After 8–12 weeks of HFD feeding, vehicle (0.5% carboxymethylcellulose) or fenofibrate was orally administrated to HFD-fed mice for 4 weeks. During fenofibrate treatment, we measured food intake twice a week. After treatment, the daily amount of food intake was calculated. As a lipodystrophic model, 12–20-week-old A-Zip/F1 mice and their WT littermates (63) were treated with 50 mg/kg/day fenofibrate or vehicle for 4 weeks. The animal care procedures and methods were approved by the Animal Care Committee of Kyoto University.

Oral glucose tolerance test and intraperitoneal insulin tolerance test

Two to 3 weeks after fenofibrate treatment, an oral glucose tolerance test was carried out by administering D-glucose (2 g/kg body wt) through a gastric feeding tube after 6 h of fasting. For the insulin tolerance test, human insulin (Eli Lilly Japan, Kobe, Japan) was injected intraperitoneally (0.75 or 1 units/kg body wt) in animals after 6-h fasting. Blood samples were collected from the tail vein before and 15, 30, 60, and 120 min after injection. The area under the curve (AUC) was calculated using the trapezoidal rule.

Cold tolerance test

Two to 3 weeks after fenofibrate treatment (50 mg/kg), rectal temperature of mice was measured at 0, 30, and 60 min after 4 °C cold exposure using a thermometer probe (T&D Corp., Nagano, Japan).

Measurement of oxygen consumption and RER

Two weeks after the initial administration, the oxygen consumption and respiratory exchange ratio (RER) of mice under

Table 5
Oligonucleotide primers used for mRNA analysis

Gene	Forward primer	Reverse primer	Gene ID
36B4	TGTGTGTCTGCAGATCGGGTAC	CTTTGGCGGGATTAGTCGAAG	11837
Fgf21	CACCGCAGTCCAGAAAGTCT	ATCCTGGTTTGGGGAGTCCT	56636
Aco	GCACCATTGCCATTCGATACA	CCACTGCTGTGAGAATAGCCGT	11430
Cpt1a	CTCAGTGGGAGCGACTCTTCA	GGCCTCTGTGGTACACGACAA	12894
Hmgcs2	AATCAGTGGAAGCAAGCTGGA	GTCCAGGGAGGCCTTCAAAA	15360
Cd36	GATGTGGAACCCATAACTGGATTCAC	GGTCCCAGTCTCATTTAGCCACAGT	12491
Ucp1	ACTGCCACACCTCCAGTCATT	CTTTGCCTCACTCAGGATTGG	22227
Pgc1a	CCCTGCCATTGTTAAGACC	TGCTGCTGTTCCTGTTTTC	19017
Cidea	ATCACAACTGGCCTGGTTACG	TACTACCCGGTGTCCATTTCT	12683
Cpt1b	CTGTTAGGCCTCAACACCGAAC	CTGTCATGGCTAGGCGGTACAT	12895
Tbx1	GGCAGGCAGACGAATGTTC	TTGTCATCTACGGGCACAAAG	21380
Tmem26	ACCCTGTCATCCCACAGAG	TGTTTGGTGGAGTCCTAAGGTC	327766
Lpl	ATCCATGGATGGACGGTAACG	CTGGATTCCAATACTTCGACCA	16956
Ppara	TCAGGGTACCACTACGGAGT	CTTGGCATTCTTCCAAAGCG	19013
Glut1	CCATCCACCACACTCACCAC	GCCCAGGATCAGCATCTCAA	20525
Fgfr1	TTGGAGGCTACAAGGTTCGC	GCGGATCGCTGTACACCTTA	14182
Klb	GGCAGGATGCCTATACGACC	GTAAACTGCGGGGAGGAGAC	83379

fed conditions were measured using an indirect calorimetric system (Oxymax; Columbus Instruments, Columbus, OH) every 9 min for 20 h. These experiments started at 4:00 pm and finished at 12:00 pm (the dark and light phases were 12 and 8 h, respectively).

Plasma characteristics

Plasma glucose, triglyceride, β-hydroxybutyrate, and free fatty acids levels were determined enzymatically using the glucose CII test and triglyceride E-test, Autokit-3-HB, and NEFA C-test (Wako Pure Chemicals, Osaka, Japan) kit, respectively. Plasma insulin, FGF21, and adiponectin levels were measured using an ELISA kit (Morinaga Institute of Biological Science, Yokohama, Japan; BioVendor, Brno, Czech Republic; R&D Systems, MN).

Insulin sensitivity analysis

Using diet-induced obese mice treated with fenofibrate for 3–4 weeks, human insulin was injected intraperitoneally (2 units/kg body wt) in mice after overnight fasting. Fifteen to 20 minutes after insulin injection, tissues were harvested from mice under anesthesia and immediately frozen in liquid nitrogen. AKT phosphorylation levels were determined by immunoblotting.

FGF21 sensitivity analysis

FGF21 sensitivity was analyzed as previously described (26, 27). Briefly, recombinant FGF21 (ATGen, Seongnam, South Korea) was injected intraperitoneally (25 μg/kg body wt). Fifteen to 20 minutes later, tissues were harvested from mice under anesthesia and immediately frozen in liquid nitrogen. ERK phosphorylation levels were determined by immunoblotting.

Hepatic lipid analysis

For the measurement of hepatic triglyceride content, the liver was homogenized in hexan/2-propanol (3:2 v/v) using a Polytron tissue grinder (Kinematica AG, Luzern, Switzerland). Lipid extracts were evaporated and resuspended in 2-propanol. The amounts of triglyceride were determined enzymatically using the Wako triglyceride E-test.

Histological analysis

For hematoxylin and eosin staining, tissues were removed from each mouse fed HFD and then fixed in 10% paraformaldehyde/PBS. After the dehydration with ethanol, the fixed samples were embedded in the paraffin. They were cut into 6-μm sections using a microtome and placed on microscope slides (Matsunami Glass, Osaka, Japan). Paraffin sections were stained with hematoxylin and eosin. For immunohistochemical analysis, tissues were fixed with Bouin solution (5% acetic acid, 9% formaldehyde, 0.9% picric acid). After embedding in the paraffin, they were cut into 6-μm sections. Sections were incubated in 1% hydrogen peroxide in methanol and then with 10% normal goat serum, rabbit antiserum against UCP1 (U6382, Sigma, 1:200), goat anti-rabbit IgG (Nichirei, Tokyo, Japan), and finally with the avidin-biotin-peroxidase complex (Nichirei) according to the conventional avidin-biotin complex method. Adipocyte sizes were measured using an image analysis pipeline developed with the EBImage (64) package of R/Bioconductor. Adaptive thresholding and the watershed method were used to separate cellular areas from the image background, and the pixel area of each adipocyte was calculated and converted to real-scale. After the automatic quantification, we checked the images for the exclusion of extreme outliers by visual inspection.

RNA preparation and quantification of gene expression

Total RNA was prepared from murine tissues using Sepasol (R)-RNA I Super in accordance with the manufacturer's protocol. Total RNA was reverse-transcribed using M-MLV reverse transcriptase (Promega, Madison, WI) in accordance with the manufacturer's instructions. To quantify mRNA expression, real-time RT-PCR was performed with a LightCycler System (Roche Diagnostics) using SYBR Green fluorescence signals as described previously (65, 66). The oligonucleotide primers were designed using a PCR primer selection program (the Virtual Genomic Center) from the GenBank™ database. The primers used for measuring mRNA expression levels of genes are listed in Table 5. To compare mRNA expression levels among the samples, the copy numbers of all transcripts were divided by those of mouse 36B4. All mRNA expression levels are represented as a ratio relative to that of the control in each experiment.

SDS-polyacrylamide gel electrophoresis (SDS-PAGE) and immunoblotting

Proteins from murine tissues were solubilized in lysis buffer (50 mM Tris·HCl, 150 mM NaCl, 1% Triton X-100, 0.5% deoxycholate, 0.1% SDS (pH 7.4), and a protease and phosphatase inhibitor mixture). The protein concentration was determined using a protein assay kit (Bio-Rad). Protein samples were subjected to SDS-PAGE followed by the transfer to PVDF membranes (Millipore, MA), which were blocked with 5% nonfat dried milk in PBS. The membranes were incubated with anti-UCP1 (U6382, Sigma, 1:1000), anti-ACO (ab59964, Abcam, MA, 1:1000), and anti-AKT (4691, 1:2000), anti-phosphorylated AKT (4060, 1:2000), anti-ERK (9102, 1:2000), anti-phosphorylated ERK (9101, 1:2000), anti-COX4 (4844, 1:1000), or anti-β-actin (4967, 1:2000) (Cell Signaling Technology, MA) diluted with blocking buffer. Proteins were detected using an ECL Western blotting detection system (GE Healthcare). For band quantification, AlphaEaseFC software (Alpha Innotec, Kasendorf, Germany) was used.

Quantification of fenofibric acid

Mice tissue samples for LC-MS analysis were homogenized in extraction solvent (ethanol). After centrifugation, the supernatant was collected as extract. This extract was used in LC-MS. LC-MS was performed using an Acquity UPLC system coupled to a Xevo QTOF-MS system (Waters, MA).

Luciferase reporter assay

PPARs ligand activities of fenofibric acid were determined by the luciferase reporter assay using chimera proteins for the GAL4 DNA-binding domain and human PPARs-ligand-binding domains as described previously (65, 66).

Statistical analysis

The results were expressed as the means and S.E. The statistical significance of differences was evaluated using Student's t tests or analysis of variance and the Tukey-Kramer test. Differences with p values of <0.05 were considered significant.

Author contributions—T. G., M. H., and T. K. designed the experiments and wrote the manuscript. T. G., M. H., M. I., H. T., M. K., and Y. L. performed the experiments. T. G., M. H., M. I., H. T., M. K., Y. L., H.-F. J., W. N., N. T., C.-S. K., R. Y., and T. K. discussed and interpreted the data. Y. A., H. T., M. K., H.-F. J., W. N., S. S., and H. M. gave technical assistance and analyzed the data. M. A.-A. and K. E. supported the A-Zip/F1 mice experiments. N. I. supported the FGF21 KO mice experiments. T. G. supervised this work.

Acknowledgments—We thank M. Komori and S. Shinotoh for technical assistance and secretarial support. We are grateful to Prof. M. Saito, Prof. K. Kimura, Prof. Y. Okamatsu-Ogura, and Dr. K. Fukano (Hokkaido University) for kind technical advice and useful discussions. This research used computational resources through the HPCI System Research Project (Project ID: hp160218).

References

1. Roberto, C. A., Swinburn, B., Hawkes, C., Huang, T. T., Costa, S. A., Ashe, M., Zwicker, L., Cawley, J. H., and Brownell, K. D. (2015) Patchy progress on obesity prevention: emerging examples, entrenched barriers, and new thinking. *Lancet* **385,** 2400–2409
2. Dietz, W. H., Baur, L. A., Hall, K., Puhl, R. M., Taveras, E. M., Uauy, R., and Kopelman, P. (2015) Management of obesity: improvement of health-care training and systems for prevention and care. *Lancet* **385,** 2521–2533
3. Evans, R. M., Barish, G. D., and Wang, Y. X. (2004) PPARs and the complex journey to obesity. *Nat. Med.* **10,** 355–361
4. Michalik, L., Auwerx, J., Berger, J. P., Chatterjee, V. K., Glass, C. K., Gonzalez, F. J., Grimaldi, P. A., Kadowaki, T., Lazar, M. A., O'Rahilly, S., Palmer, C. N., Plutzky, J., Reddy, J. K., Spiegelman, B. M., Staels, B., and Wahli, W. (2006) International Union of Pharmacology. LXI. Peroxisome proliferator-activated receptors. *Pharmacol. Rev.* **58,** 726–741
5. Goto, T., Lee, J. Y., Teraminami, A., Kim, Y. I., Hirai, S., Uemura, T., Inoue, H., Takahashi, N., and Kawada, T. (2011) Activation of peroxisome proliferator-activated receptor-α stimulates both differentiation and fatty acid oxidation in adipocytes. *J. Lipid Res.* **52,** 873–884
6. Rakhshandehroo, M., Knoch, B., Müller, M., Kersten, S. (2010) Peroxisome proliferator-activated receptor α target genes. *PPAR Res.* **2010,** 612089
7. Montagner, A., Polizzi, A., Fouché, E., Ducheix, S., Lippi, Y., Lasserre, F., Barquissau, V., Régnier, M., Lukowicz, C., Benhamed, F., Iroz, A., Bertrand-Michel, J., Al Saati, T., Cano, P., Mselli-Lakhal, L., *et al.* (2016) Liver PPARα is crucial for whole-body fatty acid homeostasis and is protective against NAFLD. *Gut.* **65,** 1202–1214
8. Schoonjans, K., Staels, B., and Auwerx, J. (1996) Role of the peroxisome proliferator-activated receptor (PPAR) in mediating the effects of fibrates and fatty acids on gene expression. *J. Lipid Res.* **37,** 907–925
9. Guerre-Millo, M., Gervois, P., Raspé, E., Madsen, L., Poulain, P., Derudas, B., Herbert, J. M., Winegar, D. A., Willson, T. M., Fruchart, J. C., Berge, R. K., and Staels, B. (2000) Peroxisome proliferator-activated receptor α activators improve insulin sensitivity and reduce adiposity. *J. Biol. Chem.* **275,** 16638–16642
10. Tsuchida, A., Yamauchi, T., Takekawa, S., Hada, Y., Ito, Y., Maki, T., and Kadowaki, T. (2005) Peroxisome proliferator-activated receptor (PPAR)α activation increases adiponectin receptors and reduces obesity-related inflammation in adipose tissue: comparison of activation of PPARα, PPARγ, and their combination. *Diabetes* **54,** 3358–3370
11. Takahashi, H., Goto, T., Yamazaki, Y., Kamakari, K., Hirata, M., Suzuki, H., Shibata, D., Nakata, R., Inoue, H., Takahashi, N., and Kawada, T. (2015) Metabolomics reveal 1-palmitoyl lysophosphatidylcholine production by peroxisome proliferator-activated receptor α. *J. Lipid Res.* **56,** 254–265
12. Inagaki, T., Dutchak, P., Zhao, G., Ding, X., Gautron, L., Parameswara, V., Li, Y., Goetz, R., Mohammadi, M., Esser, V., Elmquist, J. K., Gerard, R. D., Burgess, S. C., Hammer, R. E., Mangelsdorf, D. J., and Kliewer, S. A. (2007) Endocrine regulation of the fasting response by PPARα-mediated induction of fibroblast growth factor 21. *Cell Metab.* **5,** 415–425
13. Badman, M. K., Pissios, P., Kennedy, A. R., Koukos, G., Flier, J. S., and Maratos-Flier, E. (2007) Hepatic fibroblast growth factor 21 is regulated by PPARα and is a key mediator of hepatic lipid metabolism in ketotic states. *Cell Metab.* **5,** 426–437
14. Potthoff, M. J., Inagaki, T., Satapati, S., Ding, X., He, T., Goetz, R., Mohammadi, M., Finck, B. N., Mangelsdorf, D. J., Kliewer, S. A., and Burgess, S. C. (2009) FGF21 induces PGC-1α and regulates carbohydrate and fatty acid metabolism during the adaptive starvation response. *Proc. Natl. Acad. Sci. U.S.A.* **106,** 10853–10858
15. Ogawa, Y., Kurosu, H., Yamamoto, M., Nandi, A., Rosenblatt, K. P., Goetz, R., Eliseenkova, A. V., Mohammadi, M., Kuro-o, M. (2007) β-Klotho is required for metabolic activity of fibroblast growth factor 21. *Proc. Natl. Acad. Sci. U.S.A.* **104,** 7432–7437
16. Suzuki, M., Uehara, Y., Motomura-Matsuzaka, K., Oki, J., Koyama, Y., Kimura, M., Asada, M., Komi-Kuramochi, A., Oka, S., and Imamura, T. (2008) β-Klotho is required for fibroblast growth factor (FGF) 21 signaling through FGF receptor (FGFR) 1c and FGFR3c. *Mol. Endocrinol.* **22,** 1006–1014
17. Kurosu, H., Choi, M., Ogawa, Y., Dickson, A. S., Goetz, R., Eliseenkova, A. V., Mohammadi, M., Rosenblatt, K. P., Kliewer, S. A., Kuro-o, M. (2007) Tissue-specific expression of β-Klotho and fibroblast growth factor (FGF)

receptor isoforms determines metabolic activity of FGF19 and FGF21. *J. Biol. Chem.* **282,** 26687–26695
18. Coskun, T., Bina, H. A., Schneider, M. A., Dunbar, J. D., Hu, C. C., Chen, Y., Moller, D. E., and Kharitonenkov, A. (2008) Fibroblast growth factor 21 corrects obesity in mice. *Endocrinology* **149,** 6018–6027
19. Xu, J., Lloyd, D. J., Hale, C., Stanislaus, S., Chen, M., Sivits, G., Vonderfecht, S., Hecht, R., Li, Y. S., Lindberg, R. A., Chen, J. L., Jung, D. Y., Zhang, Z., Ko, H. J., Kim, J. K., and Véniant, M. M. (2009) Fibroblast growth factor 21 reverses hepatic steatosis, increases energy expenditure, and improves insulin sensitivity in diet-induced obese mice. *Diabetes* **58,** 250–259
20. Fisher, F. M., Kleiner, S., Douris, N., Fox, E. C., Mepani, R. J., Verdeguer, F., Wu, J., Kharitonenkov, A., Flier, J. S., Maratos-Flier, E., and Spiegelman, B. M. (2012) FGF21 regulates PGC-1α and browning of white adipose tissues in adaptive thermogenesis. *Genes Dev.* **26,** 271–281
21. Gaich, G., Chien, J. Y., Fu, H., Glass, L. C., Deeg, M. A., Holland, W. L., Kharitonenkov, A., Bumol, T., Schilske, H. K., and Moller, D. E. (2013) The effects of LY2405319, an FGF21 analog, in obese human subjects with type 2 diabetes. *Cell Metab.* **18,** 333–340
22. Adams, A. C., Yang, C., Coskun, T., Cheng, C. C., Gimeno, R. E., Luo, Y., and Kharitonenkov, A. (2012) The breadth of FGF21's metabolic actions are governed by FGFR1 in adipose tissue. *Mol. Metab.* **2,** 31–37
23. Wu, A. L., Kolumam, G., Stawicki, S., Chen, Y., Li, J., Zavala-Solorio, J., Phamluong, K., Feng, B., Li, L., Marsters, S., Kates, L., van Bruggen, N., Leabman, M., Wong, A., West, D., *et al.* (2011) Amelioration of type 2 diabetes by antibody-mediated activation of fibroblast growth factor receptor 1. *Sci. Transl. Med.* **3,** 113ra126
24. Muoio, D. M., Way, J. M., Tanner, C. J., Winegar, D. A., Kliewer, S. A., Houmard, J. A., Kraus, W. E., and Dohm, G. L. (2002) Peroxisome proliferator-activated receptor-α regulates fatty acid utilization in primary human skeletal muscle cells. *Diabetes* **51,** 901–909
25. Mashili, F. L., Austin, R. L., Deshmukh, A. S., Fritz, T., Caidahl, K., Bergdahl, K., Zierath, J. R., Chibalin, A. V., Moller, D. E., Kharitonenkov, A., and Krook, A. (2011) Direct effects of FGF21 on glucose uptake in human skeletal muscle: implications for type 2 diabetes and obesity. *Diabetes Metab Res. Rev.* **27,** 286–297
26. Hale, C., Chen, M. M., Stanislaus, S., Chinookoswong, N., Hager, T., Wang, M., Véniant, M. M., and Xu, J. (2012) Lack of overt FGF21 resistance in two mouse models of obesity and insulin resistance. *Endocrinology* **153,** 69–80
27. Fisher, F. M., Chui, P. C., Antonellis, P. J., Bina, H. A., Kharitonenkov, A., Flier, J. S., and Maratos-Flier, E. (2010) Obesity is a fibroblast growth factor 21 (FGF21)-resistant state. *Diabetes* **59,** 2781–2789
28. Dutchak, P. A., Katafuchi, T., Bookout, A. L., Choi, J. H., Yu, R. T., Mangelsdorf, D. J., and Kliewer, S. A. (2012) Fibroblast growth factor-21 regulates PPARγ activity and the antidiabetic actions of thiazolidinediones. *Cell* **148,** 556–567
29. Alberti, K. G., Jones, I. R., Laker, M. F., Swai, A. B., and Taylor, R. (1990) Effect of bezafibrate on metabolic profiles in non-insulin-dependent diabetes mellitus. *J. Cardiovasc. Pharmacol.* **16,** S21–S25
30. Jones, I. R., Swai, A., Taylor, R., Miller, M., Laker, M. F., and Alberti, K. G. (1990) Lowering of plasma glucose concentrations with bezafibrate in patients with moderately controlled NIDDM. *Diabetes Care* **13,** 855–863
31. Tenenbaum, A., Fisman, E. Z., Boyko, V., Benderly, M., Tanne, D., Haim, M., Matas, Z., Motro, M., and Behar, S. (2006) Attenuation of progression of insulin resistance in patients with coronary artery disease by bezafibrate. *Arch Intern Med.* **166,** 737–741
32. Tenenbaum, A., Motro, M., Fisman, E. Z., Schwammenthal, E., Adler, Y., Goldenberg, I., Leor, J., Boyko, V., Mandelzweig, L., and Behar, S. (2004) Peroxisome proliferator-activated receptor ligand bezafibrate for prevention of type 2 diabetes mellitus in patients with coronary artery disease. *Circulation* **109,** 2197–2202
33. Flavell, D. M., Ireland, H., Stephens, J. W., Hawe, E., Acharya, J., Mather, H., Hurel, S. J., and Humphries, S. E. (2005) Peroxisome proliferator-activated receptor α gene variation influences age of onset and progression of type 2 diabetes. *Diabetes* **54,** 582–586
34. Gälman, C., Lundåsen, T., Kharitonenkov, A., Bina, H. A., Eriksson, M., Hafström, I., Dahlin, M., Amark, P., Angelin, B., and Rudling, M. (2008) The circulating metabolic regulator FGF21 is induced by prolonged fasting and PPARα activation in man. *Cell Metab.* **8,** 169–174
35. Sidossis, L., and Kajimura, S. (2015) Brown and beige fat in humans: thermogenic adipocytes that control energy and glucose homeostasis. *J. Clin. Invest.* **125,** 478–486
36. Rousset, S., Alves-Guerra, M. C., Mozo, J., Miroux, B., Cassard-Doulcier, A. M., Bouillaud, F., and Ricquier, D. (2004) The biology of mitochondrial uncoupling proteins. *Diabetes* **53,** S130–S135
37. van Marken Lichtenbelt, W. D., Vanhommerig, J. W., Smulders, N. M., Drossaerts, J. M., Kemerink, G. J., Bouvy, N. D., Schrauwen, P., and Teule, G. J. (2009) Cold-activated brown adipose tissue in healthy men. *N. Engl. J. Med.* **360,** 1500–1508
38. Cypess, A. M., Lehman, S., Williams, G., Tal, I., Rodman, D., Goldfine, A. B., Kuo, F. C., Palmer, E. L., Tseng, Y. H., Doria, A., Kolodny, G. M., and Kahn, C. R. (2009) Identification and importance of brown adipose tissue in adult humans. *N. Engl. J. Med.* **360,** 1509–1517
39. Saito, M., Okamatsu-Ogura, Y., Matsushita, M., Watanabe, K., Yoneshiro, T., Nio-Kobayashi, J., Iwanaga, T., Miyagawa, M., Kameya, T., Nakada, K., Kawai, Y., and Tsujisaki, M. (2009) High incidence of metabolically active brown adipose tissue in healthy adult humans: effects of cold exposure and adiposity. *Diabetes* **58,** 1526–1531
40. Nagase, I., Yoshida, T., Kumamoto, K., Umekawa, T., Sakane, N., Nikami, H., Kawada, T., and Saito, M. (1996) Expression of uncoupling protein in skeletal muscle and white fat of obese mice treated with thermogenic β3-adrenergic agonist. *J. Clin. Invest.* **97,** 2898–2904
41. Barbatelli, G., Murano, I., Madsen, L., Hao, Q., Jimenez, M., Kristiansen, K., Giacobino, J. P., De Matteis, R., and Cinti, S. (2010) The emergence of cold-induced brown adipocytes in mouse white fat depots is determined predominantly by white to brown adipocyte transdifferentiation. *Am. J. Physiol. Endocrinol. Metab.* **298,** E1244–E1253
42. Shinoda, K., Luijten, I. H., Hasegawa, Y., Hong, H., Sonne, S. B., Kim, M., Xue, R., Chondronikola, M., Cypess, A. M., Tseng, Y. H., Nedergaard, J., Sidossis, L. S., and Kajimura, S. (2015) Genetic and functional characterization of clonally derived adult human brown adipocytes. *Nat. Med.* **21,** 389–394
43. Yoneshiro, T., Aita, S., Matsushita, M., Kayahara, T., Kameya, T., Kawai, Y., Iwanaga, T., and Saito, M. (2013) Recruited brown adipose tissue as an antiobesity agent in humans. *J. Clin. Invest.* **123,** 3404–3408
44. van der Lans, A. A., Hoeks, J., Brans, B., Vijgen, G. H., Visser, M. G., Vosselman, M. J., Hansen, J., Jörgensen, J. A., Wu, J., Mottaghy, F. M., Schrauwen, P., and van Marken Lichtenbelt, W. D. (2013) Cold acclimation recruits human brown fat and increases nonshivering thermogenesis. *J. Clin. Invest.* **123,** 3395–3403
45. Hiuge, A., Tenenbaum, A., Maeda, N., Benderly, M., Kumada, M., Fisman, E. Z., Tanne, D., Matas, Z., Hibuse, T., Fujita, K., Nishizawa, H., Adler, Y., Motro, M., Kihara, S., Shimomura, I., *et al.* (2007) Effects of peroxisome proliferator-activated receptor ligands, bezafibrate, and fenofibrate, on adiponectin level. *Arterioscler. Thromb. Vasc. Biol.* **27,** 635–641
46. Mazzucotelli, A., Viguerie, N., Tiraby, C., Annicotte, J. S., Mairal, A., Klimcakova, E., Lepin, E., Delmar, P., Dejean, S., Tavernier, G., Lefort, C., Hidalgo, J., Pineau, T., Fajas, L., Clément, K., and Langin, D. (2007) The transcriptional coactivator peroxisome proliferator activated receptor (PPAR) γ coactivator-1 α and the nuclear receptor PPAR α control the expression of glycerol kinase and metabolism genes independently of PPARγ activation in human white adipocytes. *Diabetes* **56,** 2467–2475
47. Ribet, C., Montastier, E., Valle, C., Bezaire, V., Mazzucotelli, A., Mairal, A., Viguerie, N., and Langin, D. (2010) Peroxisome proliferator-activated receptor-α control of lipid and glucose metabolism in human white adipocytes. *Endocrinology* **151,** 123–133
48. Calderon-Dominguez, M., Mir, J. F., Fucho, R., Weber, M., Serra, D., and Herrero, L. (2016) Fatty acid metabolism and the basis of brown adipose tissue function. *Adipocyte* **5,** 98–118
49. Hondares, E., Iglesias, R., Giralt, A., Gonzalez, F. J., Giralt, M., Mampel, T., and Villarroya, F. (2011) Thermogenic activation induces FGF21 expression and release in brown adipose tissue. *J. Biol. Chem.* **286,** 12983–12990
50. Lee, P., Linderman, J. D., Smith, S., Brychta, R. J., Wang, J., Idelson, C., Perron, R. M., Werner, C. D., Phan, G. Q., Kammula, U. S., Kebebew, E., Pacak, K., Chen, K. Y., and Celi, F. S. (2014) Irisin and FGF21 are cold-

induced endocrine activators of brown fat function in humans. *Cell Metab.* **19,** 302–309

51. Lee, P., Brychta, R. J., Linderman, J., Smith, S., Chen, K. Y., and Celi, F. S. (2013) Mild cold exposure modulates fibroblast growth factor 21 (FGF21) diurnal rhythm in humans: relationship between FGF21 levels, lipolysis, and cold-induced thermogenesis. *J. Clin. Endocrinol. Metab.* **98,** E98–E102
52. Lin, Z., Tian, H., Lam, K. S., Lin, S., Hoo, R. C., Konishi, M., Itoh, N., Wang, Y., Bornstein, S. R., Xu, A., and Li, X. (2013) Adiponectin mediates the metabolic effects of FGF21 on glucose homeostasis and insulin sensitivity in mice. *Cell Metab.* **17,** 779–789
53. Holland, W. L., Adams, A. C., Brozinick, J. T., Bui, H. H., Miyauchi, Y., Kusminski, C. M., Bauer, S. M., Wade, M., Singhal, E., Cheng, C. C., Volk, K., Kuo, M. S., Gordillo, R., Kharitonenkov, A., and Scherer, P. E. (2013) An FGF21-adiponectin-ceramide axis controls energy expenditure and insulin action in mice. *Cell Metab.* **17,** 790–797
54. Chan, S. M., Zeng, X. Y., Sun, R. Q., Jo, E., Zhou, X., Wang, H., Li, S., Xu, A., Watt, M. J., and Ye, J. M. (2015) Fenofibrate insulates diacylglycerol in lipid droplet/ER and preserves insulin signaling transduction in the liver of high fat fed mice. *Biochim. Biophys. Acta* **1852,** 1511–1519
55. Miura, Y., Hosono, M., Oyamada, C., Odai, H., Oikawa, S., and Kondo, K. (2005) Dietary isohumulones, the bitter components of beer, raise plasma HDL-cholesterol levels and reduce liver cholesterol and triacylglycerol contents similar to PPARα activations in C57BL/6 mice. *Br J. Nutr.* **93,** 559–567
56. Gonzalez, F. J., and Shah, Y. M. (2008) PPARα: mechanism of species differences and hepatocarcinogenesis of peroxisome proliferators. *Toxicology* **246,** 2–8
57. Brocker, C. N., Yue, J., Kim, D., Qu, A., Bonzo, J. A., and Gonzalez, F. J. (2017) Hepatocyte-specific PPARA expression exclusively promotes agonist-induced cell proliferation without influence from nonparenchymal cells. *Am. J. Physiol. Gastrointest. Liver Physiol.* **312,** G283–G299
58. Kharitonenkov, A., Shiyanova, T. L., Koester, A., Ford, A. M., Micanovic, R., Galbreath, E. J., Sandusky, G. E., Hammond, L. J., Moyers, J. S., Owens, R. A., Gromada, J., Brozinick, J. T., Hawkins, E. D., Wroblewski, V. J., Li, D. S., *et al.* (2005) FGF-21 as a novel metabolic regulator. *J. Clin. Invest.* **115,** 1627–1635
59. Petersen, K. F., Dufour, S., Savage, D. B., Bilz, S., Solomon, G., Yonemitsu, S., Cline, G. W., Befroy, D., Zemany, L., Kahn, B. B., Papademetris, X., Rothman, D. L., and Shulman, G. I. (2007) The role of skeletal muscle insulin resistance in the pathogenesis of the metabolic syndrome. *Proc. Natl. Acad. Sci. U.S.A.* **104,** 12587–12594
60. Lucas, E. A., Li, W., Peterson, S. K., Brown, A., Kuvibidila, S., Perkins-Veazie, P., Clarke, S. L., and Smith, B. J. (2011) Mango modulates body fat and plasma glucose and lipids in mice fed a high-fat diet. *Br J. Nutr.* **106,** 1495–1505
61. Fu, J., Gaetani, S., Oveisi, F., Lo Verme, J., Serrano, A., Rodríguez De Fonseca, F., Rosengarth, A., Luecke, H., Di Giacomo, B., Tarzia, G., and Piomelli, D. (2003) Oleylethanolamide regulates feeding and body weight through activation of the nuclear receptor PPAR-α. *Nature* **425,** 90–93
62. Hotta, Y., Nakamura, H., Konishi, M., Murata, Y., Takagi, H., Matsumura, S., Inoue, K., Fushiki, T., and Itoh, N. (2009) Fibroblast growth factor 21 regulates lipolysis in white adipose tissue but is not required for ketogenesis and triglyceride clearance in liver. *Endocrinology* **150,** 4625–4633
63. Moitra, J., Mason, M. M., Olive, M., Krylov, D., Gavrilova, O., Marcus-Samuels, B., Feigenbaum, L., Lee, E., Aoyama, T., Eckhaus, M., Reitman, M. L., and Vinson, C. (1998) Life without white fat: a transgenic mouse. *Genes Dev.* **12,** 3168–3181
64. Pau, G., Fuchs, F., Sklyar, O., Boutros, M., and Huber, W. (2010) EBImage: an R package for image processing with applications to cellular phenotypes. *Bioinformatics* **26,** 979–981
65. Goto, T., Kim, Y. I., Funakoshi, K., Teraminami, A., Uemura, T., Hirai, S., Lee, J. Y., Makishima, M., Nakata, R., Inoue, H., Senju, H., Matsunaga, M., Horio, F., Takahashi, N., and Kawada, T. (2011) Farnesol, an isoprenoid, improves metabolic abnormalities in mice via both PPARα-dependent and -independent pathways. *Am. J. Physiol. Endocrinol. Metab.* **301,** E1022–E1032
66. Goto, T., Nagai, H., Egawa, K., Kim, Y. I., Kato, S., Taimatsu, A., Sakamoto, T., Ebisu, S., Hohsaka, T., Miyagawa, H., Murakami, S., Takahashi, N., and Kawada, T. (2011) Farnesyl pyrophosphate regulates adipocyte functions as an endogenous PPARγ agonist. *Biochem. J.* **438,** 111–119

ASBMB